THE STATE UNIVERSITY OF NEW JERSEY
RUTGERS

Final Report to the

New Jersey Marine Sciences Consortium

and

New Jersey Department of Transportation
Office of Maritime Resources

EMISSIONS AND ATMOSPHERIC TRANSPORT OF PCBs AND Hg FROM STABILIZED HARBOR SEDIMENTS

Principal Investigators:
John R. Reinfelder, Gera Stenchikov, Lisa A. Totten
Department of Environmental Sciences, Rutgers University
14 College Farm Road, New Brunswick, NJ 08901

June 30, 2006

Emissions and Atmospheric Transport of PCBs and Hg from Stabilized Harbor Sediments
Final Report

Executive Summary

Project Goals, Objectives, and Approach

Previously, vertical fluxes and horizontal gradients of polychlorinated biphenyls (PCBs) and mercury (Hg) were measured by investigators from Rutgers University and Stevens Institute of Technology at a land application site for cement-stabilized dredged material (SDM) from New York Harbor located in Bayonne, New Jersey (Korfiatis et al., 2003). The results of that project pointed to gaps in our understanding of the phase partitioning of PCBs emitted from SDM, the relative importance of SDM PCB emissions to the local atmosphere compared with other sources in the New York/New Jersey metropolitan area, and the sediment side controls of PCB and Hg volatilization. The dynamics of PCB volatilization fluxes that occur as SDM cures were examined at Stevens and the results are described in a separate report (Miskewitz et al., 2005). At Rutgers, PCB sample analyses, modeling, and laboratory experiments were carried out to determine the gas-aerosol partitioning of PCBs in the Bayonne atmosphere, develop an atmospheric transport model of PCBs in the Bayonne peninsula, and further evaluate the environmental controls of Hg volatilization from SDM. The specific objectives of the Rutgers projects were to:

1. Quantify the fraction of PCBs adsorbed to airborne particles in samples previously collected at the stabilized dredged material land application site and at the NJDEP trailer site in Bayonne, NJ in order to determine if the gas-particle system is at equilibrium and assess the importance of aerosol sorption of gas-phase PCBs emitted from the stabilized sediment.
2. Utilize a RAMS/HYPACT model with measured PCB concentrations to characterize air circulation patterns and estimate the transport of PCBs from the SDM application site in Bayonne, NJ during our previous field sampling campaigns.
3. Examine in laboratory flux chamber experiments the sediment side controls of Hg volatilization from SDM.

Gas/Particle Partitioning of PCBs Near a Stabilized Dredge Material Application Site

Particle-phase PCB concentrations were determined in samples collected upwind and downwind of the SDM application site (OENJ Bayonne, see Fig. 1). Particle-phase PCB concentrations at the landfill were significantly elevated on a mass per unit volume of air basis (pg m^{-3}; 1 pg = 10^{-12} g) compared with measurements at a NJDEP air monitoring trailer in Bayonne and at Jersey City, but when these concentrations were normalized to the amount of total suspended particles (TSP) in the air, the levels were comparable between the three locations. There is no evidence in this data of consistent increases in particle-phase PCB concentrations downwind of the SDM. This is true whether the particle-phase PCB concentrations are expressed as pg m^{-3} of air or as pg μg^{-1} TSP. An evaluation of PCB gas/particle partitioning constants and vapor pressures indicates that emissions of either gas- and particle-phase PCBs from the Bayonne SDM landfill are not large enough to significantly alter the gas/particle partitioning of PCBs in this region. This occurs primarily because of the high

background concentrations of PCBs in both the gas and particle phases in Bayonne due to its location within the NYC metropolitan area. These same emissions could be significant, however, if the SDM were placed in a more remote location where the background PCB signal is lower.

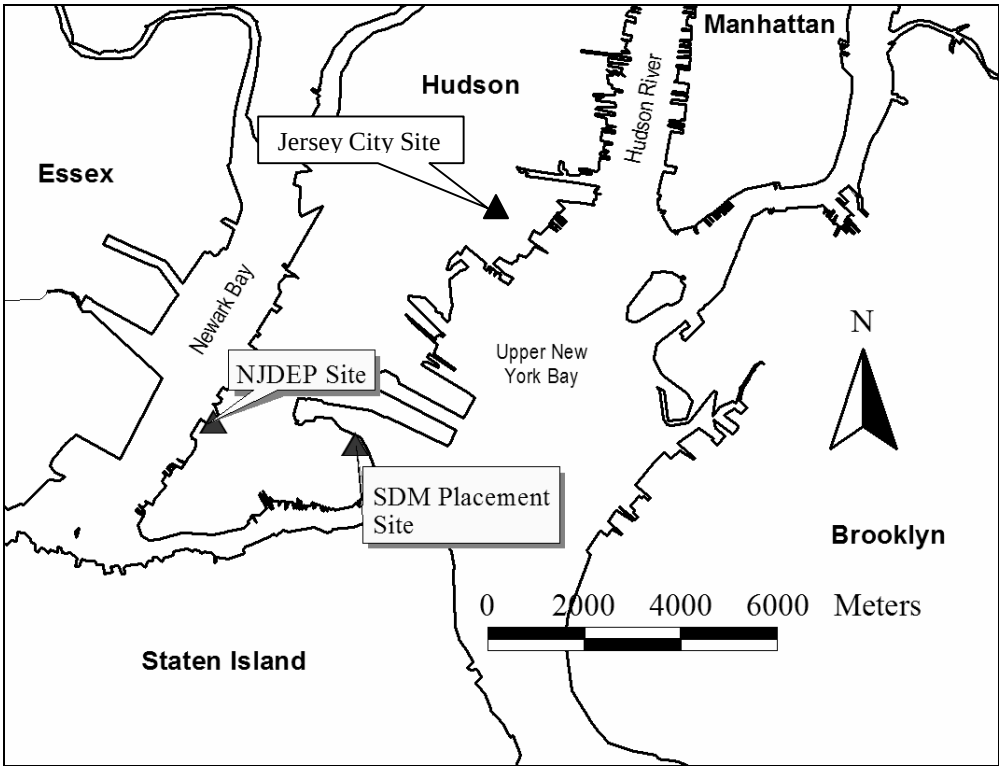

Figure 1. Aerial view of Bayonne peninsula showing the OENJ SDM application site and the NJDEP trailer.

Measurement and Modeling of Urban Atmospheric PCB Concentrations on a Small (8 Km) Spatial Scale

In order to evaluate the SDM placement site in Bayonne as a source of PCB emissions to the New York City-northern New Jersey urban atmosphere and to improve our understanding of urban sources of atmospheric PCBs generally, gas-phase PCBs were analyzed at two monitoring locations near the SDM application site (Bayonne trailer and Jersey City) for the period of December 1999 to November 2000. In addition, in order to assess the PCB emissions required to produce the measured concentrations, PCB transport was modeled using the Hybrid Particle And Concentration Transport model (HYPACT) with local meteorology generated by the Regional Atmospheric Model System (RAMS). The concentrations, congener patterns, and temporal patterns of PCBs differ dramatically at the two monitoring sites which are ~8 km apart and spikes in gas-phase PCB concentration observed at the Bayonne trailer site are not observed at

Jersey City. These results suggest that an important source of atmospheric PCBs exists within 8 km of the SDM application site.

Modeling results show that the magnitude of PCB emissions at the SDM placement site needed to produce the observed gas-phase concentrations at the SDM site (400 pg m^{-2} s^{-1}) is in good agreement with micrometeorological estimates of PCB emission fluxes based on measurements made at the SDM site during placement (570 pg m^{-2} s^{-1}; Korfiatis et al., 2003). The transport of PCB emissions of this magnitude from the SDM placement site could produce concentration spikes of only 100-200 pg m^{-3}, well below those observed at the Bayonne trailer site (400-2000 pg m^{-3}) indicating that PCB emissions from the SDM placement site have a small effect on the overall levels of PCBs measured at the Bayonne trailer and that the emissions source which produced the PCB spikes at the Bayonne trailer is either much greater than the 3 kg y^{-1} produced by the SDM placement site or much closer to the Bayonne trailer than 8 km.

The emissions of ΣPCBs needed to produce observed concentrations at the Bayonne trailer monitoring site is estimated to be on the order of 100 g d^{-1}. Extrapolation of this source magnitude to the area of New York City suggests that this urban area emits at least 300 kg of ΣPCBs to the regional atmosphere each year, an amount similar in magnitude to the flux of ΣPCBs from the Upper Hudson River into the New York/New Jersey Harbor estuary. Unfortunately, there is no way at this time to determine either the identity or exact location of this source.

Hg flux chamber experiments

The volatilization of mercury from estuarine sediments does not decrease with time as was observed for PCBs (Miskewitz et al., 2005), but is primarily controlled by light. Photochemically driven reactions at the sediment-air surface apparently lead to the reduction of Hg(II) and 20 to 40-fold increases in gaseous mercury volatilization fluxes. Cement stabilization appears to accelerate volatilization of Hg in the light perhaps by exposing photoreactive solids directly to light or increasing the surface area of the sediment through drying. The dominant role of light in controlling Hg volatilization from sediments in the laboratory flux chamber is consistent with in situ sediment-air Hg flux observations at the SDM placement site in Bayonne, NJ which were significantly correlated ($r^2 = 0.81$) with solar radiation (Goodrow et al., 2005; 2006). Decreasing the time of exposure of SDM to light during cement stabilization and placement would reduce Hg emissions to the atmosphere from this source. The photochemically-driven Hg volatilization from periodically air exposed freshwater or estuarine wetland sediments has not been directly evaluated and could be a significant flux in the atmospheric Hg cycle.

Recommendations for further study

1. Additional observational and local transport modeling studies are needed to identify and locate the major emission sources of PCBs to the New York/New Jersey metropolitan atmosphere.

2. Particle scavenging needs to be better quantified as a loss mechanism of PCBs from the major emission sources to the New York/New Jersey urban atmosphere.

3. Further examination of the effects of the intensity and wavelength of light and sediment properties (organic matter content) on Hg volatilization from sediments across a range of Hg contamination levels is needed.

4. Studies of the photoreactive/volatile forms of Hg in estuarine sediments are needed to understand the mechanism of photochemically-driven Hg volatilization and to better define the risks that unremediated Hg contaminated sediments pose to human and environmental health in NY/NJ Harbor.

5. In situ studies of sediment-air fluxes of Hg above tidally exposed and vegetated freshwater and estuarine wetlands sediments are needed to quantify this potentially important component of the Hg cycle.

Acknowledgements

This project was supported by the New Jersey Marine Sciences Consortium and the New Jersey Department of Transportation, Office of Maritime Resources. We wish to thank Michael Weinstein (NJMSC) and Scott Douglas (NJDOT) for their guidance and support. This work was made possible by the efforts of Steven J. Eisenreich, Cari L. Gigliotti, Nilesh Lahoti, Andy Sandy, and Lora Smith.

TABLE OF CONTENTS

I. Gas/Particle Partitioning of PCBs Near a Stabilized Dredge Material Land Application Site

NJ Marine Sciences Consortium (NJMSC) and NJ Department of Transportation, Office of Maritime Resources (NJDOT/OMR) recently provided funding to our research group for a study entitled: *Monitoring of PCB and Hg Air Emissions in Sites Receiving Stabilized Harbor Sediment* (Korfiatis et al., 2003). This project was designed to assess the rate and magnitude of volatilization of PCBs from a site in New Jersey where stabilized dredged material (SDM) from the NY/NJ Harbor region is applied to land (Fig. 1).

We have determined the background ambient gas-phase PCB concentrations in the air at the trailer site in Bayonne, NJ prior to and after land application of cement-stabilized sediment. The main goal of this research was to determine the extent to which the land application of these stabilized harbor sediments affects the ambient PCB concentrations in the air in Bayonne. Results from this study demonstrate that net volatilization of PCBs from the stabilized sediment is occurring. Figure 2 compares the concentrations of gas-phase ΣPCBs measured at the NJDEP trailer site (blue) with those measured at the sediment application site (red). Average concentrations at the sediment application site were found to be 1.5-2X higher than those measured at the Bayonne trailer site. Average ΣPCB concentrations during the July 2001 sampling campaign were 7128 pg m^{-3} and 3945 pg/m^3 at the sediment application site and the Bayonne trailer site, respectively. For the October 2001 sampling campaign, average ΣPCB concentrations were 2857 and 1284 pg m^{-3}, respectively. The high ambient PCB levels measured at the sediment application site relative to the local background suggest that volatilization from the sediment is a net source of atmospheric PCBs. In addition, small-scale spatial gradients in PCB concentrations demonstrate that PCBs are higher downwind of the applied sediment relative to levels measured at upwind samplers. In the worst case, gas-phase PCB concentrations downwind were 4 times upwind levels.

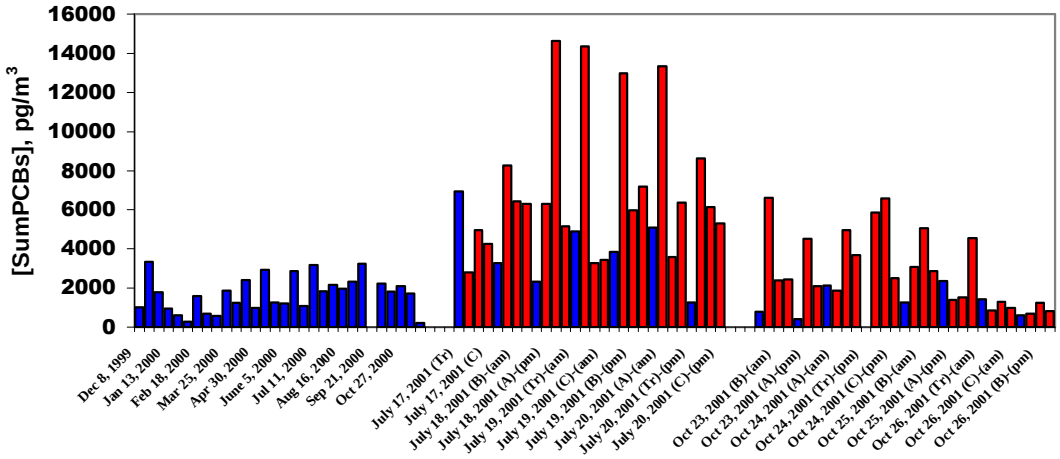

Figure 2. Concentrations of gas phase PCBs measured at the trailer site (blue) and at the sediment application site (red).

In addition to upwind and downwind measurements of PCB concentrations, a research team of scientists from Stevens Institute of Technology performed vertical PCB flux monitoring at the sediment placement site. Their data indicate that substantial amounts of PCBs are volatilized from the sediments (Korfiatis et al., 2003).

Despite the evidence that net volatilization of PCBs from stabilized sediments is occurring, it is not clear to what extent these emissions contribute to the levels of atmospheric PCBs in Bayonne and surrounding communities. During three sampling intervals, winds blew toward the northeast, in the direction of the NJDEP trailer site. On July 18, 2001 in the afternoon, gas phase ΣPCBs were 8700 pg m^{-3} at the sediment application site, but just 2300 pg m^{-3} downwind at the trailer site (Fig. 2). Similarly, on July 20, 2001, ΣPCBs were 6700 pg m^{-3} at the application site and 1300 pg m^{-3} at the trailer. During the October 2001 campaign, east/southeast wind occurred on October 23, in the morning. Concentrations at the sediment application site were 6619 pg m^{-3} downwind of the applied sediment. The ΣPCB concentration across town at the NJDEP trailer was 791 pg m^{-3}, almost a factor of 8 lower. The concentrations of PCBs measured at the trailer site under these wind conditions are low not only relative to those measured at the sediment application site, but also relative to concentrations measured at the trailer site in the year before sediment application began (Fig. 2). Thus high concentrations at the sediment application site do not directly lead to elevated PCB concentrations in the city of Bayonne, and a better understanding of the transport of PCBs from the sediment placement site is needed.

We hypothesized that the transport of gas-phase PCBs in the Bayonne area was influenced by the partitioning of PCBs onto aerosols. Gas/particle partitioning may remove a significant amount of PCBs from the gas phase during transport across the city of Bayonne. PCBs are volatilized from the stabilized sediment into the gas phase. This volatilization is likely enhanced by the elevated temperature of the sediments, which are heated by the exothermic curing of the cement additives and by solar radiation. The air directly above the sediments is also heated, but as the air masses rise, they cool, potentially inducing the PCBs in the air to condense onto airborne particles. Under light winds, air movement across the peninsula will take an hour or more, allowing time for gas/particle partitioning. Thus, in order to more accurately assess the impact of emissions of PCBs from applied sediments, it is necessary to understand the influences of gas/particle partitioning. To further this understanding, we quantified the PCBs in the atmospheric particle phase at the sediment placement and trailer sites, and examined the data for trends in gas/particle partitioning parameters in order to detect the influence of PCB emissions from the SDM on the local atmospheric PCB burden.

Sampling Methods

Details of sample collection were described in Korfiatis et al. (2003). Sample preparation, extraction and analysis procedures can be found elsewhere (Lohman et al., 2000; Gigliotti et al., 2000; Brunciak et al., 2001; Gigliotti et al., 2001; Totten et al., 2001) and will be summarized here. Air samples were collected using a modified high volume air sampler (Tisch Environmental, Village of Cleves, OH, USA) with a calibrated airflow of ~0.5 m^3 min^{-1}. Quartz fiber filters (QFFs; Whatman) were used to capture the particulate phase and polyurethane foam plugs (PUFs) were used to capture the gaseous phase. QFFs were weighed before and after sampling to determine total suspended particles (TSP).

Analytical Procedures

Samples were injected with surrogate standards before extraction. For PCBs the surrogates were 3,5 dichlorobiphenyl (PCB#14), 2,3,5-trichorobiphenyl (PCB#23), 2,3,5,6 tetrachlorobiphenyl (PCB#65), 2,3,4,4',5,6 hexachlorobiphenyl (PCB#166). Samples were extracted in Soxhlet apparati for 24 hours in dichloromethane. These extracts were then reduced in volume by rotary evaporation and subsequently concentrated via N_2 evaporation. The samples were then fractionated on a column of 3% water-deactivated alumina. The PCB fraction was eluted with hexane, concentrated under a gentle stream of nitrogen gas, and injected with internal standard containing PCB #30 (2,4,6-trichlorobiphenyl) and #204 (2,2',3,4,4',5,6,6'-biphenyl) prior to analysis by gas chromatography (GC). PCBs were analyzed on an HP 6890 gas chromatograph equipped with a ^{63}Ni electron capture detector using a 60-m 0.25 mm i.d. DB-5 (5% diphenyl-dimethyl polysiloxane) capillary column with a film thickness of 0.25 μm (Brunciak et al., 2001). Sixty peaks representing 93 congeners were quantified.

Quality Assurance

Recovery of surrogate standards, which were typically better than 71 %, was used to correct individual compound concentrations for surrogate recoveries. Field blanks and matrix spikes were used for quality control purposes. The method detection limit (MDL) for each congener was determined from field blanks by taking the mean of the mass detected in all field blanks plus three times the standard deviation about the mean. The MDL for ΣPCBs on QFF was 8.44 ng.

Results and Discussion

Table 1 summarizes the particle phase ΣPCB (n = 93 congeners) concentrations in samples collected at the SDM landfill and at the NJDEP trailer. Congener-specific data for all particle phase samples is given in Appendix 1. Particle-phase PCB concentrations varied seasonally. Highest concentrations were measured in November and lowest in May. Average ΣPCB concentrations during the July 2001 campaign were 317 and 91 pg m^{-3} at the sediment application sites and Bayonne trailer, respectively. These particle phase concentrations represented 4.4% and 2.3%, respectively, of the total atmospheric PCB burden (gas + particle). In May 2002, average ΣPCB concentrations were 108 (6% of total concentration) and 0.75 pg m^{-3} (0.08 % of total concentration), at the sediment application site and the trailer, respectively. In November 2002, average ΣPCB concentrations were 149 (9% of total concentration) and 1.5 pg m^{-3} (0.17% of final concentration), respectively. Thus the fraction of PCBs in the particle phase was generally higher at the sediment application site than at the trailer.

During virtually all sampling intervals, particle phase ΣPCB concentrations were higher at the landfill than at the trailer, in some cases by more than an order of magnitude. The concentrations at the landfill were usually higher than typical concentrations in Jersey City, NJ that are in the range of 9 to 44 pg m^{-3} (Totten et al., 2004). Particle-phase ΣPCB concentrations at the trailer averaged 25 pg m^{-3} during the intensive sampling periods, similar to the concentrations routinely observed at Jersey City. The differences in particulate phase ΣPCB concentration between the trailer and landfill were eliminated when the PCB concentrations were normalized to TSP. Such normalization results in average (± sd) particle-phase

Table 1. Summary of ΣPCB particulate phase concentration during the Bayonne 2001-2002 sampling campaigns. Samples taken upwind of the SDM are in blue, downwind samples in red.

ΣPCB concentration, pg m^{-3}	Bayonne Trailer	Sediment Site A	Sediment Site B	Sediment Site C
07/17/2001 (all day)			134	
07/18/2001 (morning	33	**91**	**111**	**47**
07/18/2001 (afternoon)	143		**842**	**56**
07/19/2001 (morning)		**449**	**498**	
07/19/2001 (afternoon)	151	**455**	**516**	**151**
07/20/2001 (morning)		**816**		**218**
07/20/2001 (afternoon)	76	**134**	**233**	
05/07/2002 (morning)	0.46	144	291	65
05/07/2002 (afternoon)	0.92		150	85
05/08/2002 (morning)	1.1	**208**	177	76
05/08/2002 (afternoon)	2.0	254		
05/09/2002 (morning)	1.0	60		**48**
05/09/2002 (afternoon)	0.55	171		**33**
05/10/2002 (morning)	0.47		66	34
05/10/2002 (afternoon)	0.44		68	42
11/12/2002 (morning)	0.69	**1237**	**147**	234
11/12/2002 (afternoon)	1.1	**106**	**128**	130
11/13/2002 (morning)	0.27	**58**	79	**54**
11/13/2002 (afternoon)			66	**78**
11/14/2002 (morning)	2.0	66	197	100
11/14/2002 (afternoon)	5.2	0.07	90	71

ΣPCB concentrations at the landfill and trailer of 0.79 (± 0.70) and 0.89 (± 0.64) pg ug^{-1}, respectively. TSP concentrations at the trailer averaged 42 ug m^{-3}, similar to observations at Jersey City (Totten et al., 2004). At the landfill, two TSP measurements were greater than 30,000 μg m^{-3}. Without these two outliers, TSP concentrations at the landfill averaged 375 μg m^{-3}. Thus increased particle-phase PCB concentrations at the landfill are a result of greater numbers of particles there. In general, the SDM does not appear to be responsible for these higher particle densities. Only three sampling intervals (7/19 afternoon, 7/20 morning, and 7/20 afternoon) display significantly elevated particle densities downwind of the SDM. Particle-phase ΣPCB concentrations normalized to TSP during these three intervals were lower downwind of the SDM than upwind. Thus for these three intervals, the SDM may be emitting significant amounts of particles, but they have a lower PCB concentration than the ambient airborne particles. The other high particle-phase PCB concentrations are due to off-site emissions of particles as well as secondary atmospheric aerosol formation.

There is no evidence in this data of consistent increases in particle-phase PCB concentrations downwind of the SDM. This is true whether the particle-phase PCB concentrations are expressed as pg per cubic meter of air or as pg per μg TSP. This suggests that gas-phase emissions of PCBs from the SDM are not large enough to significantly impact the particle-phase PCB concentrations downwind of the SDM. Closer examination of the particle-

phase PCB concentrations is therefore necessary to discern whether PCB emissions from the SDM are significant.

Flux studies have demonstrated that PCBs are emitted into the gas phase from the SDM, but it is unclear how important these emissions are to the prevailing PCB burden in the atmosphere around Bayonne. In the original study of the site we concluded that, despite relatively high gas-phase PCB concentration at the SDM site, the SDM landfill is a relatively weak source of PCBs to the City of Bayonne. The purpose of this study was to examine the gas/particle partitioning of PCBs in the vicinity of Bayonne in order to gain further insight into the relative importance of PCB emissions from the SDM landfill.

The distribution of semi-volatile compounds between the gas and particle-bound phases is the most important factor determining the removal mechanisms and residence time in atmosphere (Junge, 1977; Eisenreich et al., 1981; Cousins & Mackay, 2001; Pankow, 1987). In gas-particle partitioning, the equilibrium partitioning coefficient (K_p) describes the ratio between the particle phase concentration (C_p, pg m^{-3}) and the gas phase concentration (C_g, pg m^{-3}) of the SOC, normalized by the TSP concentration in ug/m^3 (Pankow, 1987; Pankow, 1994; Harner & Bidleman, 1998):

$$K_p = \frac{C_p}{C_g \cdot TSP} \qquad (1)$$

In theory, a plot of log K_p ($m^3/\mu g$) vs. log vapor pressure (log p_l from Falconer and Bidleman, 1994) for individual PCB congeners should yield a slope of ~ -1 when gas/particle partitioning is at equilibrium (Pankow, 1987). In this study we postulated that gas/particle partitioning will be at equilibrium for PCBs being transported in from offsite (upwind of the SDM), but will be far from equilibrium just downwind for the SDM due to gas-phase PCB emissions from the SDM. The congeners volatilized from the SDM appear to be relatively low in molecular weight (Korfiatis et al., 2003), containing 2 to 5 chlorines, and therefore have relatively high vapor pressures, putting them to the right in the lop K_p vs. lop p_l plots (see Figure 3 for an example). Increased gas-phase concentrations of these congeners would decrease their K_p value (equation 1), causing the right side of the regression line to be "dragged" downward, resulting in a slope steeper than the equilibrium value of -1. Particle phase emissions would also disturb the gas/particle partitioning of PCBs, although it is not clear how this disruption would manifest itself in terms of the log K_p vs. log p_l curve.

A summary of log K_p vs. log p_l slopes is given in Table 2. Slopes were significantly shallower than -1 in 13 of 17 intensive samples collected at the trailer site, with an average (± sd) of –0.59 (± 0.17). In previous work, we hypothesized that a significant source of atmospheric PCBs exists within about 6 km of the Bayonne trailer. If these PCBs are emitted primarily into the gas phase, their influence could explain the frequent lack of gas/particle partitioning equilibrium observed at the trailer. The average (± sd) slope at the landfill was -0.69 (± 0.15). Six of 48 samples at the trailer yielded slopes equal to –1. From this data we can conclude either that gas/particle partitioning of PCBs is usually not at equilibrium in the Bayonne area, or that slopes significantly different from –1 can still be indicative of equilibrium, as was argued by Simcik et al. (1998).

Perturbations in the gas/particle partitioning of PCBs upwind and downwind of the SDM can still be instructive even if we cannot establish that partitioning is at equilibrium at either location. We need only look for significant differences in the log K_p vs. log p_l slopes between upwind and downwind sites. In only one sampling interval (7/18/2001 afternoon) are significant differences in slopes observed upwind and downwind of the SDM (Fig. 3). During this interval,

the slope (± 95% confidence interval) was -0.72 (± 0.12) upwind and -0.40 (± 0.12) downwind. The slope at the trailer was -0.45 (± 0.13). For this sampling period, winds came from the SE, with both sites A and C acting as upwind sites and site B as the downwind site. Concentrations upwind (site C = 5153 pg m^{-3}, site A = 6298 pg m^{-3}) were as much as 2.5 times lower than downwind (14647 pg m^{-3}), suggesting that the dredge material contributed to the atmospheric burden of PCBs onsite. The particle-phase ΣPCB concentrations were 15 times higher downwind than upwind. Flux measurements were not taken during this interval, but the difference in upwind/downwind gas-phase PCB concentrations suggests that the flux was substantial. This episode appears to indicate that gas-phase emissions of PCBs from the SDM can have a significant impact on the gas/particle partitioning of PCBs, and that they do cause the slope to become more shallow, as hypothesized.

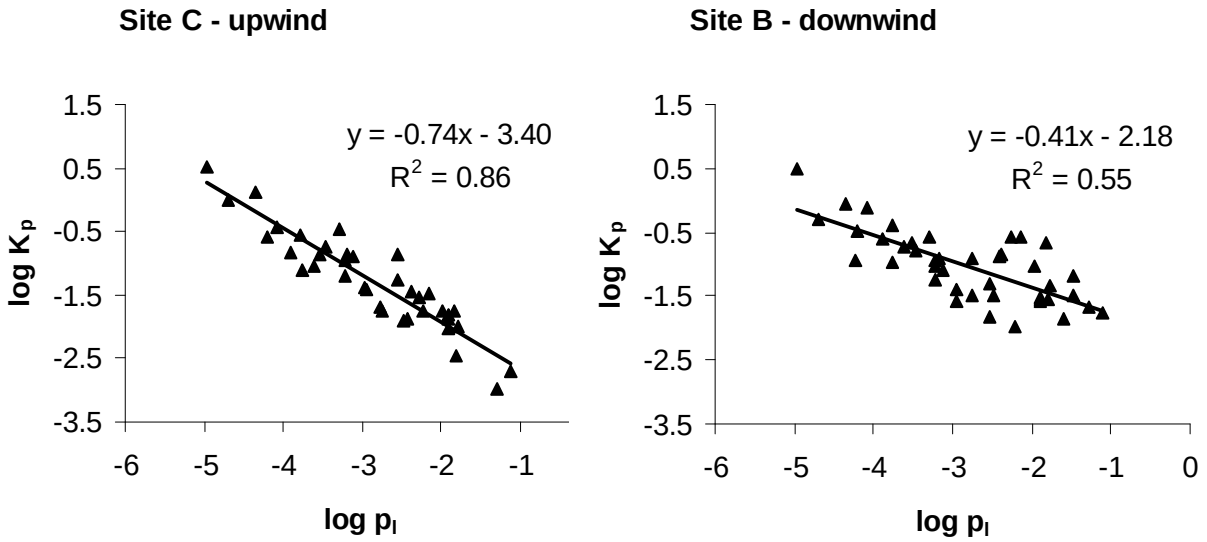

Figure 3. Gas/particle partitioning plots for PCBs at two sites near the SDM on the afternoon of 7/18/01.

Of the 21 sampling intervals listed in Table 2, only 6 coincided with flux measurements above the SDM. During the 5/7/02 (morning and afternoon) and 5/8/02 (morning) events, the ΣPCB flux was large and positive, ranging from 1987 to 2877 ng m^{-2} hr^{-1}. On 5/7/02 the wind was from the W, such that all three landfill sites were upwind. On the morning of 5/8/02, winds were from the NE, such that sample A was downwind of the SDM. There is no difference between the slopes in samples A and C. For the November intensive, fluxes were small but positive, ranging from 76 to 491 ng m^{-2} hr^{-1}. Again there are no observable differences in the slopes between upwind and downwind sites. These results may indicate that fluxes in excess of 3000 ng m^{-2} hr^{-1} are necessary to significantly affect the gas/particle partitioning of PCBs in this region due to the high background of atmospheric PCBs being transported into Bayonne from off site.

Table 2. Summary of gas/particle partitioning results during Bayonne 2001-2002 sampling campaign. Slopes, 95% confidence intervals, and R^2 values for regressions of log K_p vs. lop p_l are shown. Sites in red were downwind of the SDM, sites in blue were upwind.

	Bayonne Trailer			Site A			Site B			Site C		
Dates	**slope**	**95% CL**	**r^2**	**slope**	**95% CL**	**r^2**	**slope**	**95% CL**	**r^2**	**slope**	**95% CL**	**r^2**
7/17/2001 (all day)							-0.63	0.13	0.71			
7/18/2001 (morning)	-0.65	0.30	0.51	**-0.82**	**0.10**	**0.88**	**-0.69**	**0.12**	**0.79**	**-1.00**	**0.25**	**0.73**
7/18/2001 (afternoon)	-0.45	0.13	0.60				**-0.40**	**0.12**	**0.51**	**-0.72**	**0.12**	**0.82**
7/19/2001 (morning)				**-0.61**	**0.09**	**0.83**	**-0.40**	**0.14**	**0.45**			
7/19/2001 (afternoon)	-0.70	0.15	0.76	**-0.58**	**0.08**	**0.86**	**-0.63**	**0.09**	**0.85**	**-0.80**	**0.11**	**0.85**
7/20/2001 (morning)				**-0.57**	**0.08**	**0.83**				**-0.71**	**0.09**	**0.86**
7/20/2001 (afternoon)	-0.36	0.15	0.41	**-0.77**	**0.08**	**0.91**	**-0.72**	**0.09**	**0.88**			
05/07/2002 (morning)	-0.40	0.18	0.41	-0.35	0.11	0.53	-0.58	0.17	0.56	-0.67	0.22	0.56
5/7/2002 (afternoon)	-0.42	0.16	0.70				-0.62	0.15	0.67	-0.36	0.16	0.38
5/8/2002 (morning)	-0.54	0.13	0.67	**-0.63**	**0.09**	**0.82**				-0.62	0.18	0.60
5/8/2002 (afternoon)	-0.63	0.11	0.77	-0.52	0.17	0.49						
5/9/2002 (morning)	-0.43	0.28	0.31	-0.67	0.24	0.52				**-0.69**	**0.21**	**0.62**
5/9/2002 (afternoon)	-0.60	0.18	0.69	-0.78	0.16	0.77				**-0.88**	**0.22**	**0.68**
5/10/2002 (morning)	-0.64	0.21	0.64				-0.75	0.12	0.83	-0.76	0.20	0.64
5/10/2002 (afternoon)	-0.71	0.22	0.60				-0.72	0.11	0.84	-0.61	0.17	0.61
11/12/2002 (morning)	-0.50	0.54	0.46	**-1.00**	**0.17**	**0.81**	**-1.00**	**0.16**	**0.78**	-1.00	0.16	0.83
11/12/2002 (afternoon)	-0.81	0.23	0.64	**-0.96**	**0.17**	**0.79**	**-0.71**	**0.20**	**0.65**	-0.76	0.23	0.65
11/13/2002 (morning)	-0.76	0.46	0.73	**-0.70**	**0.15**	**0.72**	-0.63	0.15	0.69	**-0.76**	**0.16**	**0.77**
11/13/2002 (afternoon)							-0.68	0.14	0.73	**-0.68**	**0.14**	**0.71**
11/14/2002 (morning)	-0.50	0.16	0.59	-0.78	0.15	0.76	-0.63	0.15	0.68	-0.52	0.20	0.58
11/14/2002 (afternoon)	-1.00	0.20	0.83	-0.74	0.17	0.69	-0.61	0.15	0.67	-0.70	0.13	0.76

Conclusions

These results suggest that the emissions of both gas- and particle-phase PCBs from the Bayonne SDM landfill are not large enough to alter the gas/particle partitioning of PCBs in this region. This occurs primarily because of the high background concentrations of PCBs in both the gas and particle phases that occur in Bayonne due to its location within the NYC metropolitan area. These same emissions could be significant if the SDM were placed in a more remote location where the background PCB signal is lower. For example, in large portions of New Jersey, the background gas-phase PCB concentration averages 150-220 pg m^{-3}, nearly an order of magnitude lower than levels prevailing near the Bayonne landfill. The fact that perturbations in the gas/particle partitioning of PCBs downwind of the SDM are not detected does not necessarily imply that this partitioning process is unimportant. Partitioning of gas-phase PCB emissions to particles probably does have an important role to play in removing the emissions from the atmosphere, but this effect is masked by the high background levels of PCB prevailing in the atmosphere of Bayonne.

II. Measurement and Modeling of Urban Atmospheric PCB Concentrations on a Small (8 km) Spatial Scale

Measurement of atmospheric PCB concentrations has been conducted in the east coast of the US and the Great Lakes primarily for the purpose of estimating atmospheric inputs to coastal waters (Baker et al. 1997; Buehler et al. 2001; Totten et al. 2004). The New Jersey Atmospheric Deposition Network (NJADN) was established for this reason and data from this project has been used to estimate atmospheric deposition fluxes to the NY/NJ Harbor Estuary and the tidal Delaware River. NJADN as well as the Integrated Atmospheric Deposition Network (IADN), the Chesapeake Bay Atmospheric Deposition Study (CBADS), and other studies have demonstrated that atmospheric deposition can be an important and sometimes dominant source of PCBs to coastal waters, and that atmospheric PCB concentrations are generally greater in urban areas than in rural or suburban areas (Baker et al. 1997; Buehler et al. 2001; Totten et al. 2004). This observation suggests that urban emissions of PCBs support the regional background concentrations observed in rural areas and control the atmospheric deposition of these compounds. Thus it is important to understand the sources of urban PCBs so that they can be effectively controlled (Gingrich and Diamond 2001, Harner et al. 2004).

A further impetus for understanding urban PCB sources comes from the requirement for Total Maximum Daily Loads (TMDLs) in many aquatic systems in the US. For example, the Delaware River TMDL model, using NJADN data, estimates that the atmospheric load of ΣPCBs is ~4,000 g day^{-1} (Fikslin and Suk, 2003), exceeding the TMDL by an order of magnitude.

The cost and logistics of maintaining atmospheric deposition networks such as NJADN and IADN typically limit the scope of the project to a small number of monitoring sites, mostly located at regional sites and tens to hundreds of km apart. For example, the IADN was originally designed to have one remote site for each of the Great Lakes and was later expanded to include two urban sites in Chicago at the Illinois Institute of Technology (IIT) and the University of Illinois at Chicago (UIC). Concentrations of PCBs at UIC were found to be about twice those at IIT, although congener patterns at the two sites were virtually identical (Basu et al. 2004). The NJADN included at various times 13 monitoring locations in New Jersey, eastern Pennsylvania, and Delaware. Even so, the NJADN spaced monitoring locations as far apart as possible. When only one monitoring station is placed in each city, the tacit assumption is made that this single station accurately characterizes the atmospheric concentrations of PCBs for the whole city.

From December 1999 to November 2000, atmospheric PCBs were measured at two monitoring locations about 8 km apart within the New York City metropolitan area: Jersey City and Bayonne. The Bayonne monitoring site was established to determine the background atmospheric concentrations of PCBs in Bayonne prior to land application of stabilized dredged material from the NY/NJ Harbor at a landfill in Bayonne, NJ (Korfiatis et al. 2003). Here we examine the similarities and differences in PCB concentrations and patterns at these two sites in order to improve our understanding of urban sources of atmospheric PCBs. In order to assess the emissions required to produce the measured concentrations, the Regional Atmospheric Model System (RAMS) was used to generate local meteorology simulations, and the Hybrid Particle And Concentration Transport model (HYPACT) was used to model transport of the emitted PCBs. This represents the first report of the use of the RAMS/HYPACT model system to examine atmospheric concentrations of persistent organic pollutants (POPs).

Experimental Section

Bayonne and Jersey City lie on a peninsula separating Newark Bay from the Upper New York Bay and Hudson River (Fig. 1). The Jersey City site was operated on the grounds of the Liberty Science Center, in a grassy area less than ~30 m from the Hudson River. The Bayonne site was located on top of an air monitoring trailer operated by the NJ Department of Environmental Protection, parked at the edge of the football stadium of Bayonne High School, within ~30 m of Newark Bay.

The entire peninsula is heavily urbanized and industrialized (Fig. 1). Due west lies the city of Newark, home to Port Newark, Newark Airport, and a major incinerator. Just north of Newark lies the New Jersey Meadowlands, home to more than 10 current or former landfill areas. Newark Bay represents the confluence of the Passaic and Hackensack Rivers and receives effluent from at least four paper mills. Newark Bay and the Hudson River are hydraulically linked and tidally mixed. The waters surrounding the peninsula contain about 10-20 ng L^{-1} ΣPCBs (dissolved plus particulate) (Litten, 2003) and are therefore potential sources of atmospheric PCBs (Totten et al. 2001). The rivers feeding this area (the Hudson, Passaic, and Hackensack Rivers) all contain similar levels of PCBs.

Details of sample collection, preparation, extraction and analysis can be found elsewhere (Totten et al. 2001 and 2004; Brunciak et al. 2001) and will be summarized here. Air samples (24 hours) were collected at 12 day frequencies using a modified high volume air sampler (Tisch Environmental, Village of Cleves, OH, USA) with a calibrated airflow of ~0.5 m^3 min^{-1}. Quartz fiber filters (QFFs; Whatman) were used to capture the particulate phase and polyurethane foam plugs (PUFs) were used to capture the gaseous phase. Particle-phase PCBs were not quantified at Bayonne because it was assumed that any PCBs emitted from the stabilized sediment would be emitted into the gas phase, and because the particle phase typically contains <10% of the atmospheric PCB burden. The samples were extracted using a Soxhlet apparatus, cleaned up using 3% deactivated alumina, and analyzed for PCBs by electron capture detection (ECD). Three surrogates were used to quantify the recovery of PCBs: PCBs 23, 65, and 166. Surrogate recoveries were used to correct PCB concentrations, averaged better than 80%, and were never below 50% at both sites.

Results and Discussion

The results from several years of measurements at the Jersey City site are presented in Totten et al. (2004). During the year of simultaneous sampling, average (± standard deviation) gas-phase ΣPCB concentrations were 1600 ± 880 pg m^{-3} at Bayonne and 930 ± 460 pg m^{-3} at Jersey City. These concentrations are typical of those measured over a longer time period at Jersey City (averaging 1260 pg m^{-3} from October 1998 to January 2001). They are significantly higher than the concentrations measured at more remote regions of New Jersey, where gas-phase ΣPCBs typically average 150-220 pg m^{-3} (Totten et al. 2004). ΣPCB concentrations were more variable at Bayonne (Fig. 4). At Bayonne, the ΣPCB concentrations are similar (the ratio of the Bayonne to the Jersey City concentration is between 0.5 and 2) on 15 of the 25 simultaneous sampling days, and dissimilar (Bayonne/Jersey City >2) on 10 days. These periodic spikes in concentration raise the PCB levels at Bayonne on average by about 1500 pg m^{-3}.
Congener patterns at the two sites were usually similar with an R^2 greater than 0.7 for 20 of the 25 paired samples. The days with the most dissimilar congener patterns occurred on days when the relative percent differences in the ΣPCB concentrations ranged from 130% to 11%,

suggesting that differences in congener patterns do not necessarily lead to differences in ΣPCB concentrations. There was no clear correlation between low correlation coefficients or spikes in concentration at Bayonne (Table 3) and any natural phenomena, including wind directions, back trajectory endpoints (NOAA HYSPLIT), precipitation patterns, or tidal cycles (neap vs. spring tides). The only meteorological variable to display a significant ($R^2 = 0.19$, $p = 0.028$) correlation with the Bayonne/Jersey City PCB ratio was the average wind speed, with the ratio being higher when wind speeds were greater. The absolute concentrations at Bayonne were not correlated with wind speed, although at Jersey City, ΣPCB concentrations decreased when wind speeds increased ($R^2 = 0.24$, $p = 0.01$), possibly due to dilution.

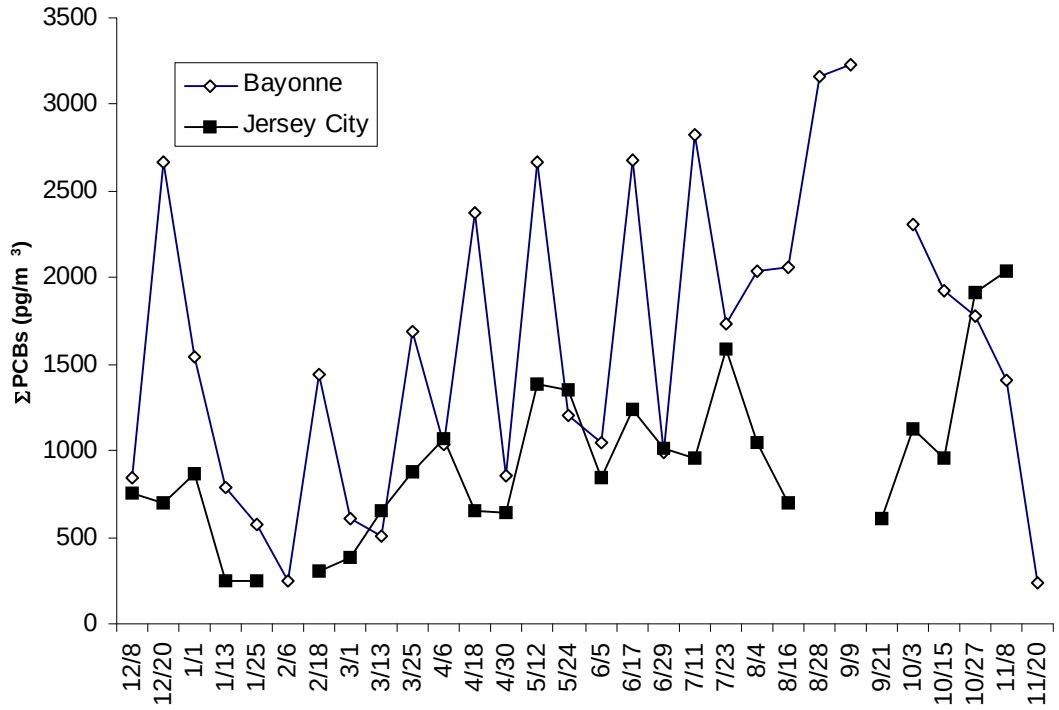

Figure 4. Gas-phase ΣPCB concentrations at the Bayonne trailer and Jersey City from December 1999 to November 2000.

The temperature (*T* in Kelvin) dependence of the gas-phase PCB partial pressures (*p* in atm) was investigated by application of the Clausius-Clapeyron equation:

$$\ln p = \frac{a}{T} + b \qquad (1)$$

where *a* and *b* are a constants. This approach has been used by many researchers, with steeper slopes thought to indicate closer sources (see Wania et al. 1998 and Carlson and Hites, 2005 for reviews). Carlson and Hites (2005) suggest that the ~25 data points used here are insufficient to

accurately determine the temperature dependence of PCBs over the long term at these sites. The goal of this analysis, however, is not to determine long-term differences in PCB dynamics, but to assess short-term differences in PCB behavior. For this purpose, 25 data points are sufficient to reveal significant differences in PCB dynamics.

Table 3. ΣPCB concentration, ratio of these concentrations at Bayonne to Jersey City, wind direction and speed, and correlation coefficient (R^2) for the congener patterns at Bayonne and Jersey City.

	ΣPCBs (pg m^{-3})		BA/JC	Wind Direction	Average Wind Speed	Congener Pattern
Date	**Bayonne**	**Jersey City**	**ratio**	**(degrees)**	**(m s^{-1})**	**R^2**
12/8/99	845	750	1.1	240	4.8	0.76
2/20/99	2672	702	3.8	190	9.0	0.92
1/1/00	1545	868	1.8	200	3.8	0.74
1/13/00	793	250	3.2	320	16	0.94
1/25/00	573	250	2.3	310	16	0.34
2/6/00	247			250	12	
2/18/00	1444	308	4.7	45	8.8	0.64
3/1/00	605	378	1.6	170	5.5	0.85
3/13/00	501	657	0.8	250	7.1	0.62
3/25/00	1685	873	1.9	220	6.6	0.88
4/6/00	1031	1071	1.0	300	12	0.96
4/18/00	2370	657	3.6	40	15	0.16
4/30/00	861	639	1.3	330	13	0.74
5/12/00	2669	1387	1.9	50	7.8	0.74
5/24/00	1205	1351	0.9	270	9.2	0.56
6/5/00	1052	850	1.2	80	11	0.85
6/17/00	2674	1242	2.2	265	9.1	0.71
6/29/00	991	1008	1.0	210	5.7	0.71
7/11/00	2821	954	3.0	310	10	0.78
7/23/00	1728	1582	1.1	225	5.8	0.74
8/4/00	2032	1047	1.9	270	7.5	0.80
8/16/00	2065	695	3.0	320	10	0.76
8/28/00	3165			80	8.7	
9/9/00	3225			40	5.6	
9/21/00		609		280	11	
10/3/00	2307	1121	2.1	280	7.1	0.84
10/15/00	1928	952	2.0	80	6.5	0.83
10/27/00	1777	1911	0.9	70	6.0	0.92
11/8/00	1403	2034	0.7	40	3.5	0.86
11/20/00	242			250	10	

At Jersey City, the Clausius-Clapeyron regressions were significant ($p < 0.05$) for all PCB congeners and co-eluting congener groups, with R^2 values ranging from 0.30 to 0.89. The slopes (*a*) values derived displayed a stronger correlation ($p < 10^{-5}$; $R^2 = 0.35$) with the log of the hypothetical subcooled liquid vapor pressure (log p_L from Falconer and Bidleman 1994) than the slopes at Bayonne. In contrast, the Clausius-Clapeyron regressions were not significant ($p > 0.05$) for 4 congener groups at Bayonne, and the R^2 values, even for the regressions that were significant, were generally weaker than at Jersey City and weakest for congeners with log vapor pressures ranging from –2.2 to –3.5 Pa (i.e. PCBs eluted between and including PCBs 66+95 and PCB 185 and containing 3-6 chlorines). Data from Bayonne for days with no observed PCB spike displayed higher Clausius-Clapeyron correlation coefficients for the congeners between 66+95 and 185 than the "spike" days. This indicates that the "background" PCB concentrations are primarily driven by processes that are correlated with temperature, such as passive volatilization from contaminated land, vegetation, or water surfaces, but the process that is driving the PCB spikes at Bayonne is not driven by temperature. Days with PCB spikes at Bayonne generally did not display positive residuals for the Clausius-Clapeyron regressions at Jersey City, indicating that the spike at Bayonne did not elevate the concentration at Jersey City significantly above the concentration that would be predicted by temperature.

A chemical mass balance model was applied to the PCB concentration data to elucidate the Aroclor pattern of the atmospheric PCBs and to determine whether the PCB spikes were due to emissions of an identifiable Aroclor. The congener compositions from Frame et al. (1996) of the 4 Aroclors produced in highest volumes (Brown, 1994) were multiplied by their sub-colled liquid vapor pressures (Falconer and Bidleman, 1994) to convert them to the congener profile expected in the atmosphere, and then expressed as a percent of the total composition. Aroclor 1016 was not used in this model because it represents a distillation of Aroclor 1242. These congener patterns were then fit via a least-squares regression to the congener pattern of each sample (again expressed as a percent of total), with the constraint that the coefficients *a*, *b*, *c*, and *d* must be greater than or equal to zero:

$$C_i = a \cdot C_{1242} + b \cdot C_{1248} + c \cdot C_{1254} + d \cdot C_{1260} \qquad (2)$$

Where C_i is the normalized concentration of congener *i* in the atmospheric sample, and C_{12xx} is the normalized concentration of congener *i* in Aroclor number 12xx. Aroclors patterns 1248b and 1254b (Frame et al. 1996) were used in the analysis because they consistently gave better fits to the data that the alternative samples of the same Aroclor. Aroclor 1242 was usually present, and the other Aroclors were always present in the samples. The average Aroclor profiles of the two sites were similar, with the percentages of Aroclors 1242, 1248, 1254, and 1260 respectively being 10%, 44%, 21%, and 14% at Jersey City and 14%, 28%, 26%, and 15% at Bayonne. The residual (that part of the congener pattern not described by the Aroclors) averaged 10% at Jersey City and 17% at Bayonne. There were no obvious differences in Aroclor composition between the days with PCBs spikes at Bayonne and the days without, nor between the Bayonne Aroclor composition and the Jersey City composition on the days with spikes. This suggests that the source of the PCBs spikes at Bayonne does not consist of a single Aroclor, but is a mixture of several Aroclors.

This analysis has suggested that one or more active sources of PCBs existed near the Bayonne site during 1999-2000 and may still exist. It also provides some information as to the type and location of the source. The source is probably within ~8 km of the Bayonne monitoring

site, since 8 km away at Jersey City, the signal from this source is not measurable. In addition, it is logical to assume that the source is closer to the Bayonne site than the Jersey City site. Because there is no correlation between PCB spikes at Bayonne and any natural phenomenon (temperature, tides, precipitation), the PCB spikes are thought to arise from anthropogenic activities that could include periodic disposal or trans-shipment of PCB-contaminated waste, and illegal disposal of PCB-containing materials. Finally, the analysis of congener patterns suggests that the source contains a mixture of PCBs, as opposed to being comprised of a single Aroclor. Unfortunately the area around Bayonne contains dozens of sites fitting this description, and additional data collection would be needed to determine which of the many suspects is responsible for the PCB spikes at Bayonne.

The dredging of NY/NJ Harbor to maintain, and in some cases deepen, the shipping channels is of enormous economic importance to the region, but is environmentally problematic due to the relatively high levels of PCBs and other contaminants in the surficial sediments of the Harbor (Adams et al. 1998) . During the period of sample collection, the confined aquatic disposal facility in Newark Bay (NBCDF) was the only disposal option for this dredge material. For this reason, dredging and disposal records provided by NJDOT Office of Maritime Resources were examined to determine whether the NBCDF could be a source of atmospheric PCBs to Bayonne. The records indicate that neither dredging nor disposal occurred in this region during the first half of 2000, suggesting that the NBCDF is not the source of the PCB spikes observed at Bayonne.

How large must the emissions of PCBs be to support the atmospheric concentrations of PCBs observed at Bayonne? To answer this question, a modeling exercise was conducted in which three possible locations for the source of PCBs were examined, the CDF site in Newark Bay, New York City (NYC) and the landfill where sediment dredge material (SDM) from the Harbor was applied to land. The model utilized the Regional Atmospheric Model System (RAMS) and the Hybrid Particle and Concentration Transport model (HYPACT). These models were recently applied by the authors to an investigation of the fate of the plume of contamination emanating from the World Trade Center in lower Manhattan resulting from the terrorist attacks of September 11, 2001 (Stenchikov et al., submitted).

RAMS version 4.3 was used to downscale the Eta Weather Prediction Model forecast (Mesinger et al. 1988; Rogers et al. 1996) conducted with spatial resolution of about 32 km. The downscaled meteorological fields were used in the HYPACT model for fine grid transport and deposition calculations. To account for a multiscale structure of the transport here we conducted calculations in three nested domains centered on the Bayonne peninsula (Fig. 5). The large parent domain is necessary to accommodate mesoscale structures to be downscaled in two smaller nested domains centered at the same central point covering areas of 54 km × 54 km and 10.5 km × 10.5 km, respectively (Fig. 5). The spatial resolution of Grids 1, 2, and 3 is, respectively, 4 km × 4 km, 1 km × 1 km, and 0.25 km × 0.25 km and number of grid points are 75 × 75, 54 × 54, and 42 × 42. The vertical grid is nonuniform, contains 39 levels starting from 10 m surface layer and reaching 1700 m at the top of the domain at the altitude of 16 km.

The original RAMS land elevation and vegetation cover data sets are of 1-km resolution that is sufficient for calculations of mesoscale circulation but is not enough for our application. To conduct finer-resolution simulations in the metropolitan area we adopted high-resolution National Land Cover Dataset (NLCD) and National Elevation Data (NED) from the United States Geological Survey (USGS) (http://edcwww.cr.usgs.gov/doc/edchome/ndcdb/ndcdb.html). NED has a resolution of 1 arc-second or about 30 m for conterminous United States.

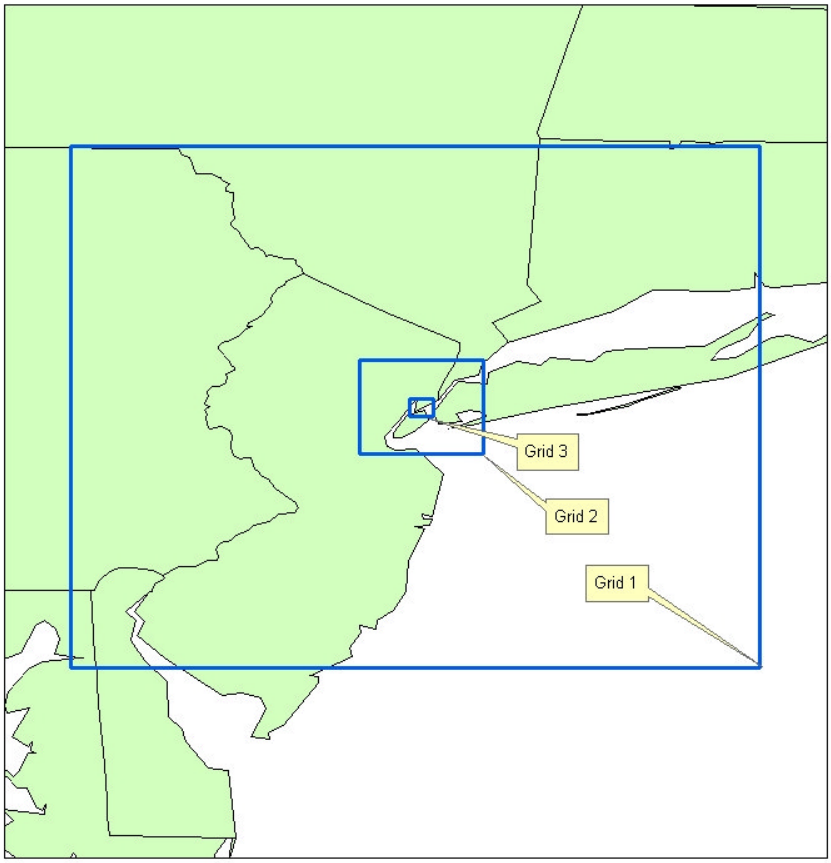

Figure 5. Model domains for the RAMS/HYPACT simulations used in the Bayonne PCB transport model.

NLCD is a multilayer and multi-source database that contains 30-m resolution 21-class land classification for territory of the Unites States in the form of visual images. The Visual Basic script was used to read pixel values and to produce a digital data file. Further we converted the NLCD classes to Olson type classes (http://edcdaac.usgs.gov/glcc/globdoc1_2.html) and then produced a LEAF2 database for RAMS.

The original RAMS Sea Surface Temperature (SST) is based on climatologically averaged monthly mean 1° × 1° resolution data set of Reynolds et al. (2002). However, fine-scale transport of pollutants in this area is almost certainly affected by sea breezes initiated by the actual land/sea temperature contrast. Therefore in our simulations we have used real-time SST with better spatial resolution. For this purpose we acquired 1 km resolution multi-channel Advanced Very High Resolution Radiometer satellite retrievals (Bernstein 1982) from the Marine Remote Sensing Laboratory of the Rutgers Institute for Marine and Coastal Sciences.

These data were processed to remove the effect of clouds seen in the instantaneous retrievals and produce the 3-day SST composites.

The meteorology simulations are driven by the initial and boundary conditions that we developed using the objective analysis package belonging to RAMS. These objectively analyzed fields are calculated using 3-hourly Eta model operational analysis (Mesinger et al. 1988; Rogers et al. 1996) . The Eta Model data were provided by the National Center for Environmental Prediction (NCEP) in gridded binary (GRIB) format on a horizontal grid with the spatial resolution of 32 km. The objectively analyzed 3-hourly fields are used to constrain the flow near the boundaries of the grid 1 domain using nudging type Davies (1976) boundary conditions with the nudging time of 30 minutes at the 5-grid-cell boundary belt. In addition, to keep the flow close to observation during the entire period of simulations we nudged horizontal velocity, potential temperature, and Exner function in the interior of the domain with much larger nudging time of 12 hours to let small-scale high-frequency disturbances to develop. The RAMS simulations were conducted using radiative scheme of Harrington (1997), turbulent closure of Mellor and Yamada (1982), and driving fields calculated using Eta fields. The meteorological fields were saved every 30 minutes.

In an attempt to identify possible sources of the PCB concentrations observed at the Bayonne trailer, we modeled the transport of pollutants from three hypothetical sources, the Bayonne landfill, the NBCDF site, and New York City. Pollutant transport was calculated off-line using the Lagrangian model HYPACT version 1.2 and meteorological output from RAMS. Three unit PCB sources emitting in the 1-m surface layer were included in calculations of PCBs at the Bayonne landfill, the NBCDF, and New York City. The NBCDF location was chosen because it possessed the characteristics attributed to the PCB source: it is within 8 km of the Bayonne trailer and is closer to the Bayonne site than the Jersey City site. The NYC site was chosen because it is reasonable to assume that NYC emits significant quantities of gas-phase PCBs. To distinguish the effects of all these three sources their emissions were treated as different tracers. PCBs at the Bayonne landfill and the NBCDF were assumed to be emitted from a square area of 500 m × 500 m. The hypothetical source in NYC was assumed to have a rectangular shape of 4 × 10 km covering the lower part of Manhattan. The actual magnitude of these sources is not known, therefore we conducted calculations with unit sources of 1g s^{-1} and later scaled the emission to fit the observed concentrations, assuming a linear relationship between emission and measured concentration. For this initial modeling effort, PCBs were assumed to exist in the gas phase only and were not subjected to hydroxyl radical reactions. This assumption is reasonable since at equilibrium only about 10% of the total atmospheric burden of PCBs is typically in the particle phase. This assumption is further justifiable considering the short distances involved, which imply travel times of a few hours at most. Also, these assumptions provide the highest, or worst-case scenario, estimates of atmospheric PCB concentrations.

HYPACT simulations were conducted for six periods during which intensive sampling of atmospheric PCBs was conducted at three locations within the landfill and at the NJDEP trailer during placement of SDM at the landfill in Bayonne (Korfiatis et al. 2003). For purposes of calculating the emissions necessary to produce the observed concentrations at the Bayonne trailer, we used results obtained for October 23-26, 2001 which are representative of the typical airflow patterns in this region.

Observed wind series measured by Automated Surface Observation Stations (ASOS) at the JFK and Newark airports available from National Climate Data Center (NCDC)

(http://www4.ncdc.noaa.gov/cgi-win/wwcgi.dll?wwdi~ASOSPhotos) were compared with RAMS output to assess model accuracy (Fig. 6). The simulations captured time variations of wind directions and magnitude fairly accurately at both locations.

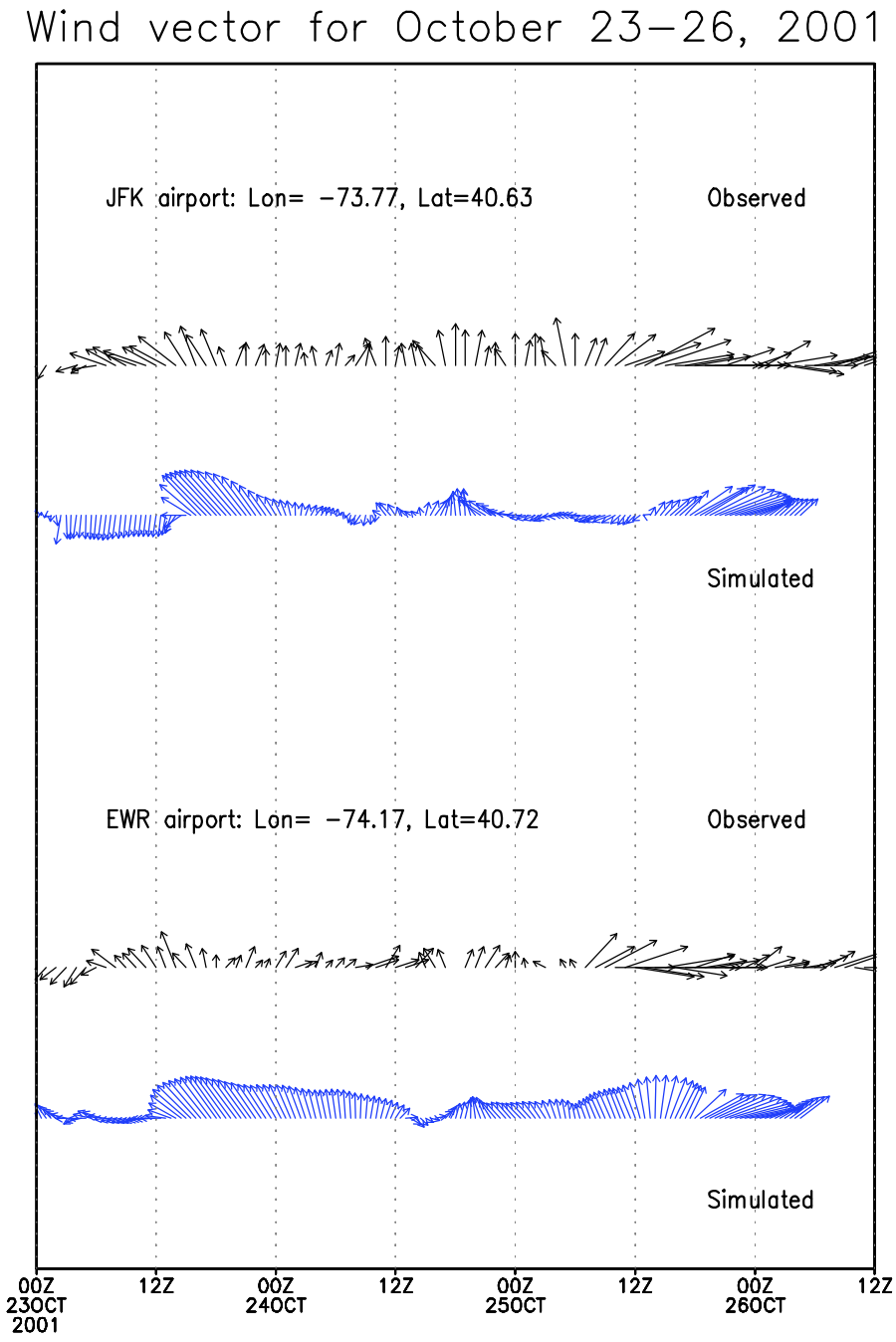

Figure 6. Observed winds (black) at JFK and Newark Airports and simulated (blue) winds at the same locations from the RAMS model at an altitude of 5 m.

Figure 7 depicts observed and simulated PCB concentrations at the SDM and trailer sites for the October, 2001 model period. In interpreting this figure it is important to remember that the measured concentrations represent integrated 4-hour measurements, while the lines are instantaneous predicted concentrations. PCB concentrations predicted at two locations (SMD landfill and trailer) are shown as they are produced by 3 different sources located at SDM landfill, NBCDF, and NYC, as was discussed above. The magnitude of each source needed to produce concentrations of the same magnitude as observed at a particular location was estimated. To our knowledge, this is the first time RAMS/HYPACT or similar atmospheric model has been used to examine emissions of Persistent Organic Pollutants on a local scale, and the results provide powerful insights into the magnitude of emissions necessary to produce the PCB levels

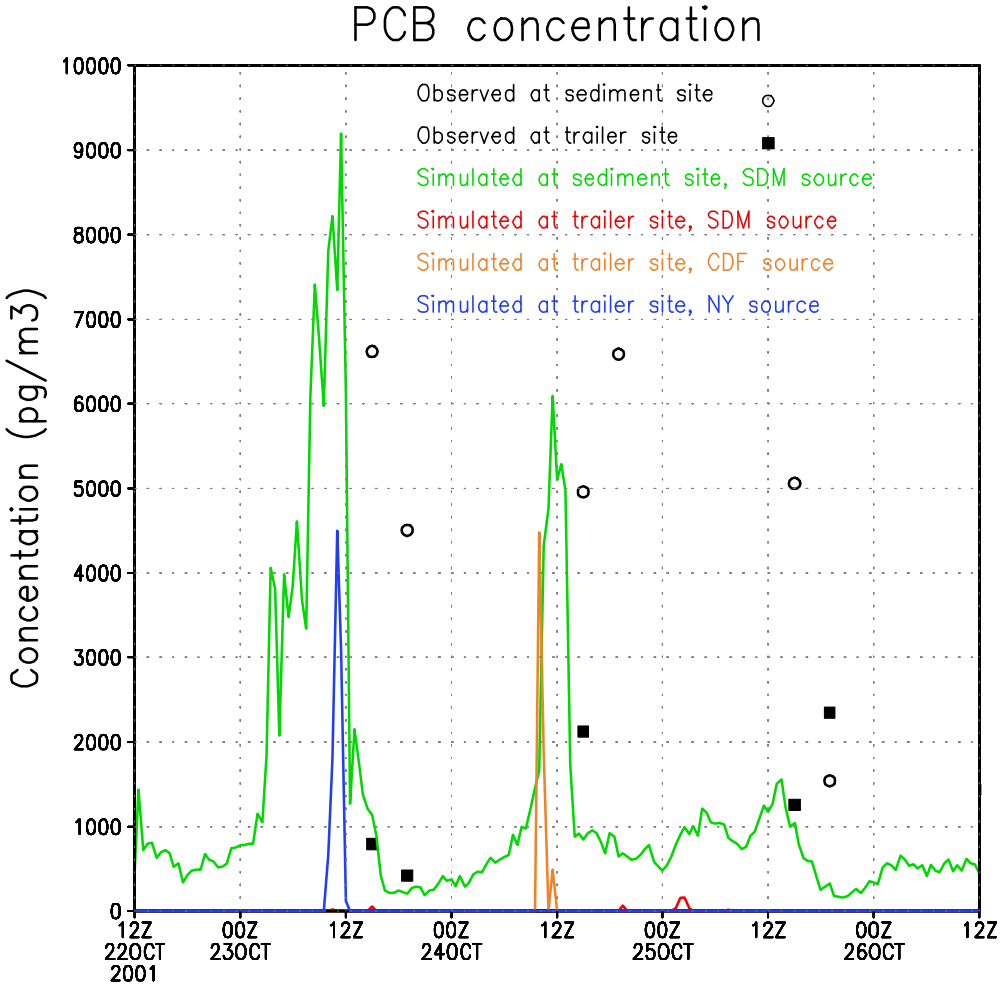

routinely measured in urban areas.

Figure 7. Solid lines depict HYPACT predicted gas-phase ΣPCB concentrations at the landfill (green) or trailer (all other colors) sites, assuming a source at the SDM placement site (Bayonne Landfill) (green and red), Newark Bay CDF (orange), or New York City (blue). The emissions rates used to generate these lines are 10^{-4} g s^{-1} at the SDM landfill (green and red lines), 10^{-3} g s^{-1} at the NBCDF (orange) and 10^{-3} g s^{-1} at NYC (blue). Measured gas-phase ΣPCB concentrations

are shown for the trailer (filled squares) and SDM placement site (open circles).

At the sediment site we have shown only concentrations transported from the local SDM site (green curve). The magnitude of PCB emissions at the SDM site that produces concentrations of 4000-7000 pg m^{-3} as was observed at the landfill (open circles; see Korfiatis et al. 2003) is 10^{-4} g s^{-1} or about 3 kg y^{-1}. Dividing this emission rate by the surface area over which sediment was spread on that particular day yields a surface flux equal to 400 pg m^{-2} s^{-1}. This value is in good agreement with the PCB volatilization flux (570 pg m^{-2} s^{-1}) estimated from micrometeorological measurements at the SDM site (Korifatis et al. 2003). The transport of PCB emissions of this magnitude from the SDM source could produce concentration spikes of 100-200 pg m^{-3} at the Bayonne trailer (red curve). These instantaneous levels are well below observed 4-hour integrated concentrations at this site that range from 400-2000 pg m^{-3} (closed squares), suggesting that the emissions from SDM placement activities at the Bayonne landfill have a small effect on the overall levels of PCBs measured at the Bayonne trailer. That a source of 3 kg of PCBs per year produces a minimal PCB signal 8 km away suggests that the levels of PCBs routinely measured in urban areas are produced by emissions that are orders of magnitude greater. It also suggests that the emissions which produced the PCB spikes at Bayonne are either much greater than 3 kg y^{-1} or that the source is much closer than 8 km.

It is useful to examine the impact that emissions from NYC have on the PCB levels measured at Bayonne, because although we do not know the magnitude of emissions from NYC, it is safe to assume that such emissions do exist. Of course, NYC cannot be the source of the PCB spikes measured at Bayonne because, due to its location, its emissions would have a greater impact at the Jersey City site than at the Bayonne site. Nevertheless, Figure 7 indicates that PCB emissions from NYC on the order of 32 kg y^{-1} are not observable at the Bayonne site most of the time. Only on the relatively rare occasions when the winds blow directly from NYC to Bayonne (for example, Oct 23 at noon) can this level of emissions produce a measurable PCB concentration at Bayonne.

Could emissions from the NBCDF explain the PCB spikes measured at the trailer? PCB concentrations resulting at the trailer site from the NBCDF (orange curve) are also shown in Figure 7. The magnitude of the source needed to produce short-term spikes in PCB concentrations that are similar in magnitude to those observed at the trailer is about 10^{-3} g s^{-1}. Are these emissions plausible? For the NBCDF, the emissions represent some fraction of the total mass of PCBs deposited into the facility during the measurement period. During the second half of 2000, approximately 160,000 cubic yards of dredge material were placed into the CDF. If the density of this material is assumed to be 500 kg m^{-3} and the PCB concentration is assumed to equal that of Newark Bay surface sediments (~750 ppb, Adams et al. 1998), then about 45 kg of PCBs were placed into the NBCDF during this 6-month period. At 10^{-3} g s^{-1}, about 16 kg of PCBs would have volatilized out of the NBCDF during this period, or one-third of the total PCB inventory in the sediments placed in the NBCDF. Given the long residence times of PCBs in sediments, this rate of volatilization seems unreasonably high. This calculation supports the conclusion that the NBCDF cannot be the source of the PCB spikes observed at Bayonne.

In addition to horizontal concentrations, it is useful to examine the vertical distribution of PCBs (Fig. 8). Vertical concentration profiles of unreactive contaminants are determined by three factors: the height of the emissions, the distance from the source, and the structure of the boundary layer. For PCBs, we assume that all emissions occur at ground level. The relatively low temperatures during the period of the modeling (October) will tend to create stable boundary conditions, trapping the ground level emissions below the boundary layer. During hotter months

when the boundary layer is less stable or during front passage or convective events, greater

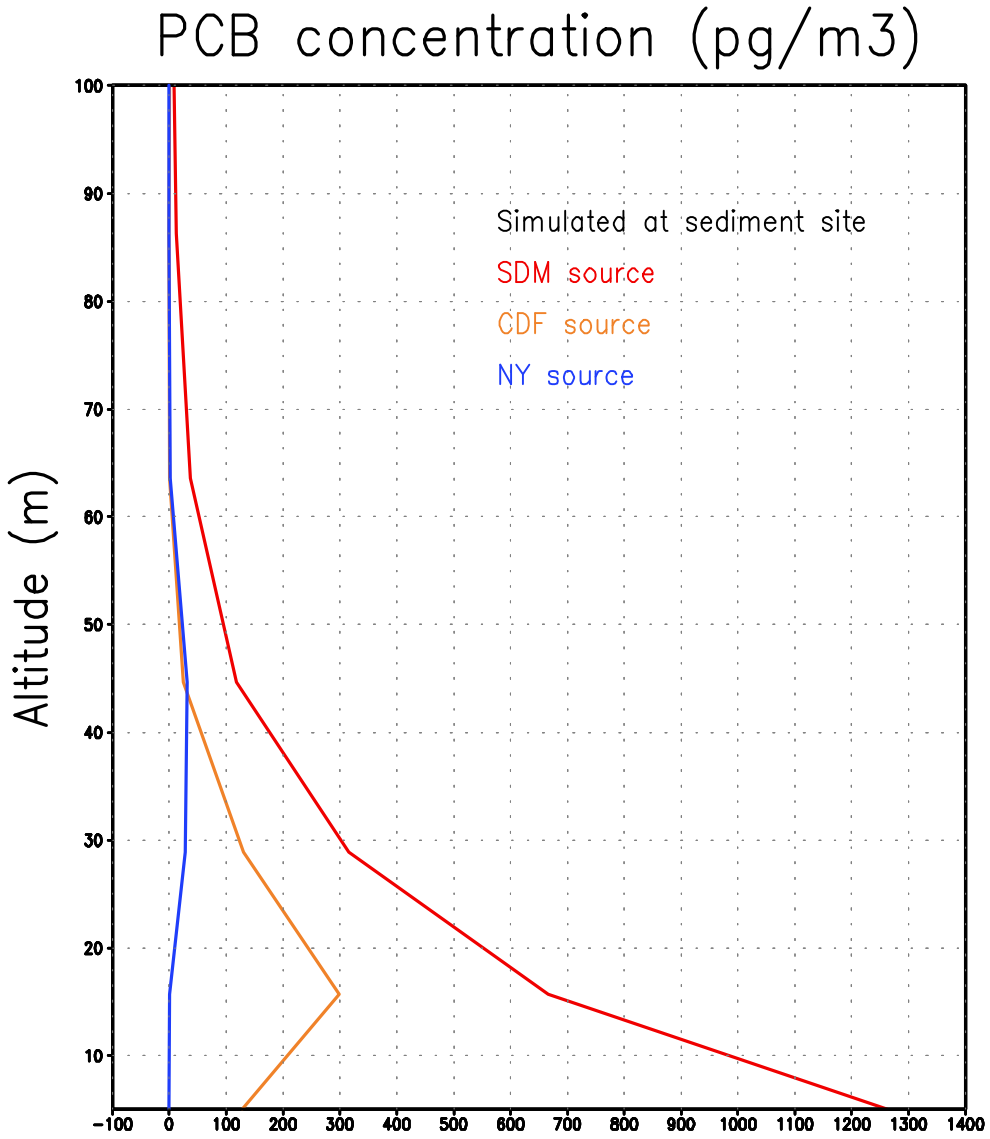

Figure 8. Vertical distribution of PCBs predicted by the RAMS/HYPACT model at the SDM landfill during October 23-26, 2001 assuming emissions at the SDM (red), NYC (blue), and CDF (orange).

turbulent mixing will facilitate the transport of PCBs above the boundary layer, where they will have greater potential for long-range transport (Stenchikov et al. 2005) . Maximum PCB concentrations occur at ground level only when the receptor (monitoring site) is directly above the emission point (in our scenario, at the SDM). When the receptor is removed from the source by a few km (NYC or NBCDF), the PCB concentrations reach a maximum 15-45 km above ground level. Farrar et al. (2005) measured the vertical distribution of PCBs in the urban

atmosphere of Toronto up to 360 meters. These researchers noted a profile characteristic of ground level emissions and a stable boundary layer (concentrations are highest at ground level and decrease with height) for some PCB congeners, but ΣPCBs were generally well mixed up to 360 m. These observations are in good agreement with our model results, which indicate that PCB concentrations do not necessarily display obvious vertical gradients below the urban boundary layer, which is generally above 400 m, unless the receptor is immediately above the emissions source.

Our modeling indicates that PCB concentrations drop to zero at ~100 m, whereas Farrar et al. (2005) measured significant PCB levels at 360 m. This discrepancy results from at least two factors: the stability of the October boundary layer, and the small number and relatively low intensity of the PCB sources in the model. Instability in the boundary layer would lead to a concentration profile that is relatively constant with height. Additional sources added to the RAMS/HYPACT model, especially sources located farther from the receptor, would increase PCB concentrations at heights above 100 m. This fact, coupled with the observations of Farrar et al. (2005), suggest that urban areas such as NYC and Toronto probably emit far more PCBs to the atmosphere than the ~70 kg y^{-1} used in our model.

How high might the urban emissions of PCBs be? The model results can be used to calculate the minimum total PCB emissions necessary to maintain the concentrations measured at the Bayonne trailer and at the nearby Jersey City NJADN site. The modeled urban source flux of 10^{-3} g s^{-1} represents a load of about 32 kg y^{-1} to the atmosphere of the region, and is barely observable 8 km away. Thus a source of this magnitude is sufficient to contaminate the air in only about a 6 km radius, or about 100 km^2. If a source of this magnitude is located within every 100 km^2 block of New York City (785 km^2), combined they would generate a relatively constant gas-phase PCB concentration of about 1000 pg m^{-3} at ground level throughout the City, similar to the levels observed at the Bayonne trailer and the Jersey City NJADN site. This PCB concentration is reasonable given that it is similar to the average gas-phase PCB concentrations measured in urban areas such as Camden, NJ (Totten et al. 2004) and Chicago, IL (Basu et al. 2004). This corresponds to PCB emissions on the order of ~800 g d^{-1}, or ~300 kg y^{-1}. For comparison, the largest single source of PCBs to the water column, the Hudson River, is estimated to contribute about 300 kg y^{-1} to the NY/NJ Harbor (Farley et al. 1999). This represents a minimum estimate because it does not consider the removal of PCBs from the lower atmosphere due to dry deposition and hydroxyl radical reactions.

III. Mercury Flux Chamber Studies

Natural and anthropogenic sources contribute gaseous elemental mercury (Hg°) to the regional and global atmosphere. Although mercury emissions from point sources can be identified and potentially controlled, emissions from contaminated ecosystems and terrestrial surfaces are widely distributed and largely unquantified. Recent attention has been drawn to the importance of Hg volatilization from soils and terrestrial vegetation (Lindberg et al., 1998; Gustin, 2003). In particular, the volatilization of Hg from naturally enriched or industrially contaminated soils and sediments is seen as an important pathway in the redistribution of mercury on watershed to global scales (Ferrara et al., 1998; Gustin et al., 2000). This redistribution of mercury pollution may increase the exposure of aquatic ecosystems to reactive Hg which can be methylated (Compeau and Bartha, 1985; Gilmour et al., 1992), enriched in aquatic and terrestrial food chains (Mason et al., 1996; Burger and Gochfeld, 1997; Watras et al., 1998; Gnamus et al., 2000) and act as a potent neurotoxicant in birds and mammals (Clarkson, 2002). In addition, the re-emission of Hg previously accumulated in soils and sediments via atmospheric deposition is an important aspect of the mercury cycle in non-point source impacted areas that needs to be accounted for in order to accurately quantify net atmospheric inputs of mercury to watersheds and the aquatic ecosystems they supply (Gustin, 2003). Global mercury budgets indicate that 50% of deposited mercury is re-emitted to the atmosphere (Bergan et al., 1999; Mason and Sheu, 2002)**,** but only order-of-magnitude estimates of terrestrial emissions are available (Schroeder and Munthe, 1998; Scholtz et al., 2003).

The global average natural emission rate of mercury from land surfaces has been estimated to be approximately 1 ng m^{-2} h^{-1} (Fitzgerald and Mason, 1996), but field studies have shown that naturally enriched and anthropogenically contaminated soils and waters emit mercury vapor at much higher rates (Lindberg et al., 1979, 1995a,b; Carpi and Lindberg, 1997, 1998; Gustin, 1998; Gustin et al., 1996, 2000). For example, measured Hg fluxes range from 8 to 45 ng m^{-2} h^{-1} for natural soils (Poissant and Casmir, 1998; Carpi and Lindberg, 1998; Engle et al., 2001) and from 10 to 1500 ng m^{-2} h^{-1} for contaminated soils (Lindberg et al., 1995b; Carpi and Lindberg, 1997; Ferrara et al., 1998). Since mercury volatilization from land is dominated by the flux of elemental Hg (Kim and Lindberg, 1995), environments that favor the reduction of Hg(II), such as highly productive wetlands, are likely to support even higher Hg° emissions. Indeed, with few exceptions (Lee et al., 2000), relatively high evasive fluxes of Hg have been measured in natural wetland ecosystems (30-3000 ng m^{-2} h^{-1}, Kozuchowski and Johnson, 1978; Leonard et al., 1998; Lindberg et al., 2002).

Upland placement of dredged materials from navigation channels in the New York/New Jersey Harbor is currently being used to manage sediments deemed inappropriate for open water disposal. Although upland placement sites are equipped with engineering controls (leachate collection and/or barrier walls), little is known of the potential impacts of this approach to air quality. Sediment-air fluxes of Hg at the SDM placement site estimated by the micrometeorological technique (–13 to 1040 ng m^{-2} h^{-1}; sediment to air fluxes being positive) were similar to those for anthropogenically-enriched surfaces and were significantly correlated ($r^2 = 0.81$) with solar radiation (Goodrow et al., 2005). The goal of this project was to determine the sediment side control of Hg volatilization from cement-stabilized sediments in controlled laboratory flux chambers.

Initial experiments

The fluxes of Hg from Newtown Creek sediments were monitored along with those of PCBs under controlled laboratory conditions using a large wind tunnel flux chamber constructed at Stevens Institute of Technology (Fig. 9). The Stevens wind tunnel permitted chemical flux measurements from 1 m^2 of sediment under laminar or turbulent flow conditions. The intake of the wind tunnel was a 6.4:1 (area basis) contraction section designed to ensure parallel flow in the test section. After passing through the contraction section the air passed through a two meter long section in which the flow profile is allowed to develop. The air then passed over the sediment in a 2 m long by 0.5 m wide by 10 cm high section. The air was then pulled through another contraction to the sampling section. In the sampling section, a small sample of air was drawn off for semi-continuous gaseous Hg and water vapor analysis.

Figure 9. Wind tunnel used to determine sediment-air fluxes of PCBs and Hg from SDM.

Total gaseous mercury (TGM) concentrations in the laboratory where the flux chamber was initially set up were well above background outdoor concentrations. Concentrations of mercury in this lab ranged from 7 to 40 ng m^{-3} (Figs. 10 and 12) whereas background mercury concentrations in Bayonne, NJ are about 2 ng m^{-3} (Korfiatis et al., 2003). Elevated mercury concentrations in the inflow air of the Stevens flux chamber obscured or reversed mercury volatilization and generally low sediment-air mercury fluxes (<25 ng m^{-2} h^{-1}) or absorption of Hg by the sediment (negative fluxes) were observed measured in all experiments (Table 4).

The volatilization of Hg from Newtown Creek sediment was dependent on temperature. Thus the highest fluxes of Hg out of the sediments were observed over the course of a high temperature excursion during the February 2004 experiment (Fig. 11). Mercury volatilization may also depend on the concentration of mercury in the sediment, but over the relatively small

range of mercury concentrations in the two batches of Newtown Creek sediments used in the six Stevens flux chamber experiments (4.2 and 7.2 μg g^{-1}), no relationship between Hg volatilization and sediment Hg content was observed (Table 4). Another factor controlling the difference in mercury concentration between in and outside of the flux chamber experiment is the air flow rate which, if too high relative to the volatilization rate, could dilute any volatilized mercury below detection by difference with the concentration of Hg in the inflow air. Turning off the flow of air through the chamber and, as a result, stopping the movement of air into the flux chamber laboratory from adjacent rooms, resulted in significantly higher concentrations of gaseous mercury inside the flux chamber with respect to outside the chamber (Fig. 12). This result suggests that mercury volatilization occurred at a relatively slow rate in the Stevens flux chamber.

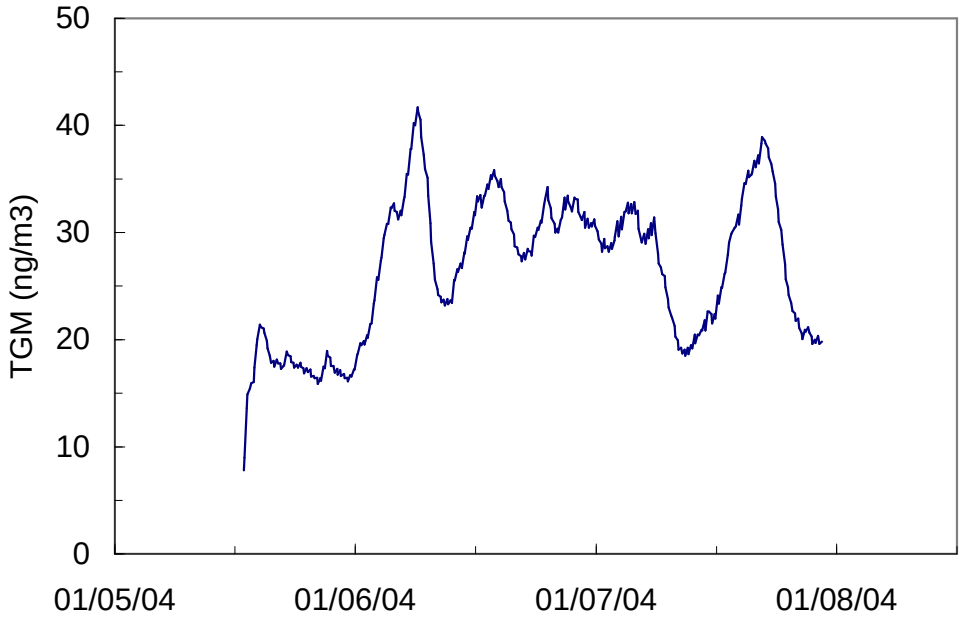

Figure 10. Gaseous mercury concentrations in the flux chamber laboratory, January 2004.

Table 4. Gaseous mercury fluxes from Newtown Creek sediment measured at Stevens Institute. Positive fluxes are from sediment to air.

Date	Cement (%)	Sediment Hg (μg g^{-1} dry wt)	Temp (°C)	heat flux (W m^{-2})	Hg fluxes (ng m^{-2} h^{-1})
Dec-03	0	4.2	12 to 19	low or <0	-150 to +100
Jan-04	8	4.2	14 to 18	low or <0	-130
Feb-04	4	4.2	13 to 17	9 to 15	-75 to +150
March 8-04	8	7.3	19	6 to 10	-200 to 0
March 15-04	4	7.3	20	10	-150 to 0
March 23-04	0	7.3	19	-20 to -40	-300 to 0

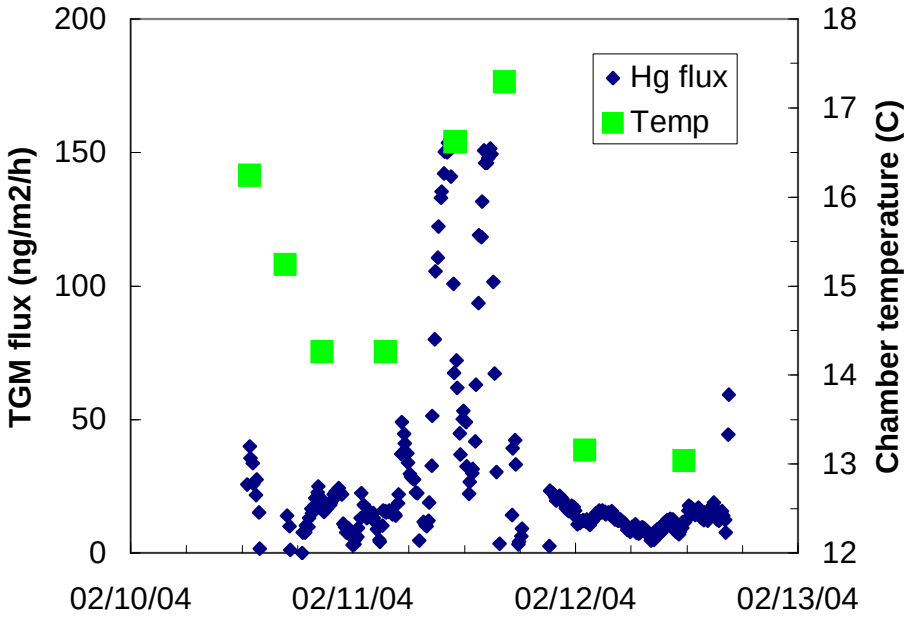

Figure 11. Estimated total gaseous mercury (TGM) fluxes from the first batch of Newtown Creek sediment treated with 4% Portland cement, February 2004.

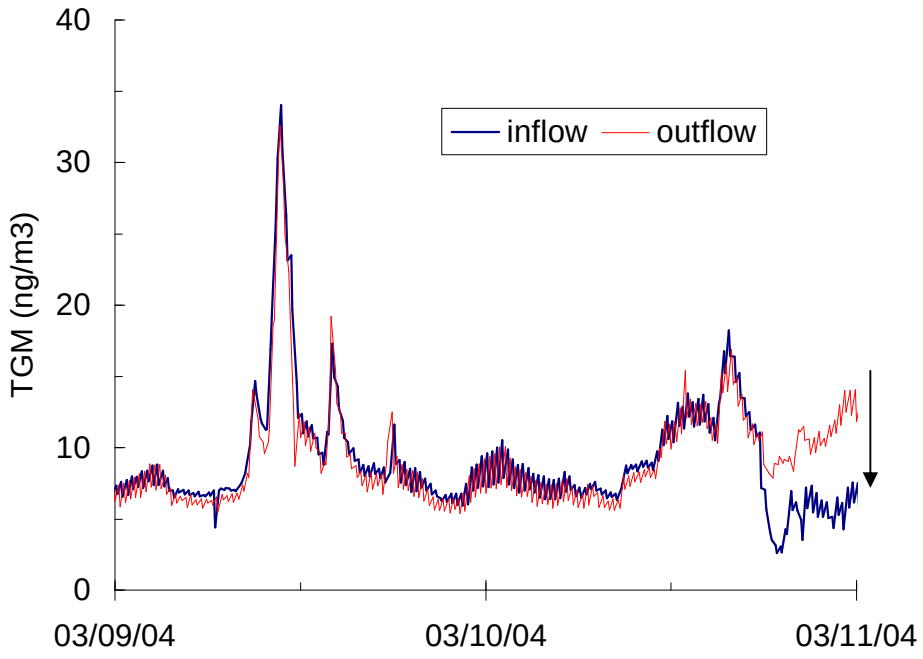

Figure 12. Total gaseous mercury (TGM) concentrations in the inflow and outflow air of the flux chamber during the March 9, 2004 experiment with the second batch of sediment. Air flow

through the chamber (and as a result, into the chamber laboratory from other rooms in the building) was stopped in the afternoon of March 10 (arrow).

In June 2004, the Stevens flux chamber was moved to a laboratory in a different building, but TGM levels were even higher (25 to 50 ng m^{-3}) than in the first location. Consequently, TGM fluxes were not measured during sediment flux chamber experiments in the summer of 2004 and it was decided that a smaller flux chamber in which mercury-free air could be used as the inflow air would be constructed for use at Rutgers.

Experiments with the new flux chamber

The new sediment flux chamber (Fig. 13) was constructed of transparent acrylic and included a 100 cm long, 10 cm wide, and 5 cm deep sediment drawer (sediment surface area = 0.1 m^2) that fits into a 120 cm long sealed chamber with 10 cm flow establishment sections at both ends and a 1 cm headspace above the sediment surface. Mercury-free inflow air supplied by a Tekran zero air generator flows first through the 10 cm flow establishment section, then over 1 m of sediment, and finally through the second 10 cm flow establishment section. All of the exit air is drawn directly into a Tekran continuous gaseous mercury analyzer at a sampling rate of 1.5 L min^{-1}. With a cross-sectional area of 10 cm^2 for the headspace above the sediment and an air velocity of 2.5 cm s^{-1}, the chamber will accommodate laminar air flow with an estimated Reynolds number of 1.7.

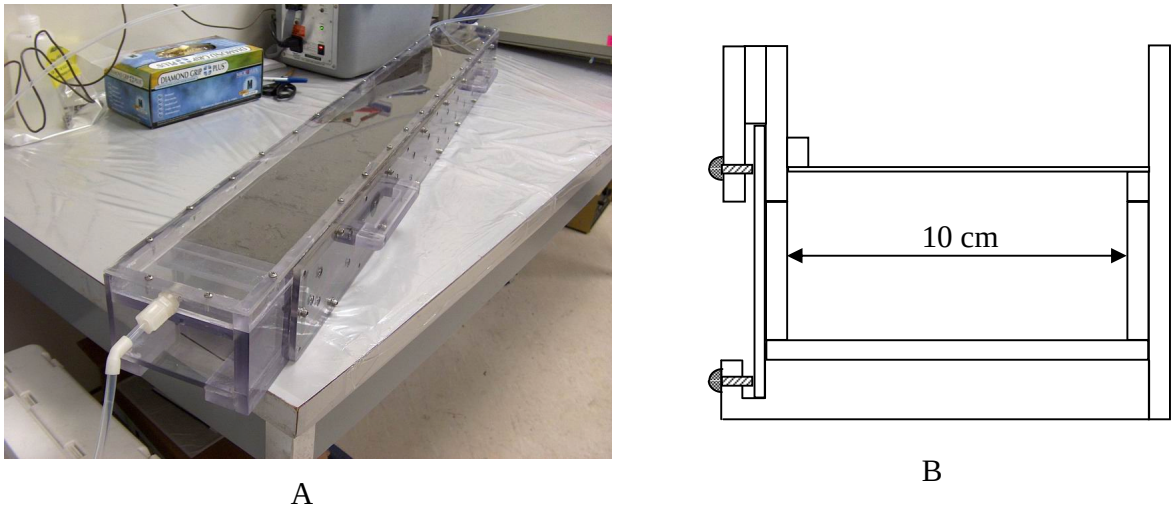

A B

Figure 13. Sediment flux chamber with sediment inside viewed from the mercury-free air inlet end (A) and a schematic cross-section (B).

Sediment flux experiments were carried out over 24 to 72 h by monitoring the concentration of gaseous mercury in air leaving the sediment-filled chamber under laminar flow conditions. Five to 30-minute gaseous mercury concentrations (ng m^{-3}) were converted to mercury fluxes (ng m^{-2} h^{-1}). During initial tests of the sealed flux chamber without sediment, mercury concentrations in the chamber were below detection demonstrating that no mercury leaked into the chamber from the laboratory under normal operating conditions.

Flux chamber experiments were conducted with both unstabilized sediments and cement-stabilized sediment with up to 6% cement by weight. Additional experiments were carried out to assess the role of light on mercury volatilization. Sediment used in these experiments was collected in October 2004 from air-exposed (low tide) mudflats in the Berry's Creek canal at a location where sediment mercury concentrations range from 20 to 40 μg g^{-1} (Cardona et al., in prep.) and stored at 4ºC until use. Approximately 5.5 L of homogenized sediment was placed in the sealed sediment flux chamber and brought to experimental temperature (17.5±1ºC) in a controlled temperature room. Once equilibrated to the experimental temperature, the flux chamber was supplied with mercury-free air (≤ 0.5 psi above atmospheric pressure, ambient humidity) under laminar flow conditions and TGM concentrations were measured in the outflow air. Two 40 watt fluorescent bulbs provided 80 μmol m^{-2} s^{-1} visible light and 0.8 μmol m^{-2} s^{-1} UV-A to the chamber and were turned on and off over one hour and 12 h intervals. TGM measurements, accuracy and reproducibility are described in Goodrow et al., 2005.

Results with unstabilized Berry's Creek sediments indicate that photochemical reactions are important to the volatilization of mercury from sediments (Fig. 14). In the dark, TGM in the sediment flux chamber built up to 0.57 ± 0.14 ng m^{-3}, significantly lower than the "urban background" concentration measured in Bayonne, NJ (2.2 ng m^{-3}; Korfiatis et al, 2003; Goodrow et al., 2005) and that measured in the controlled temperature room outside the flux chamber (2.8 ± 0.2 ng m^{-3}). In the light, however, the concentration of TGM in the flux chamber built up to 12 ± 1.0 ng m^{-3}, about 20 times higher than that in the dark. Sediment temperatures were the same in the light and the dark indicating that the increase of TGM observed in the light was dependent on photochemical reactions. Light had no effect on TGM concentrations in the controlled temperature room outside the flux chamber or within the empty flux chamber.

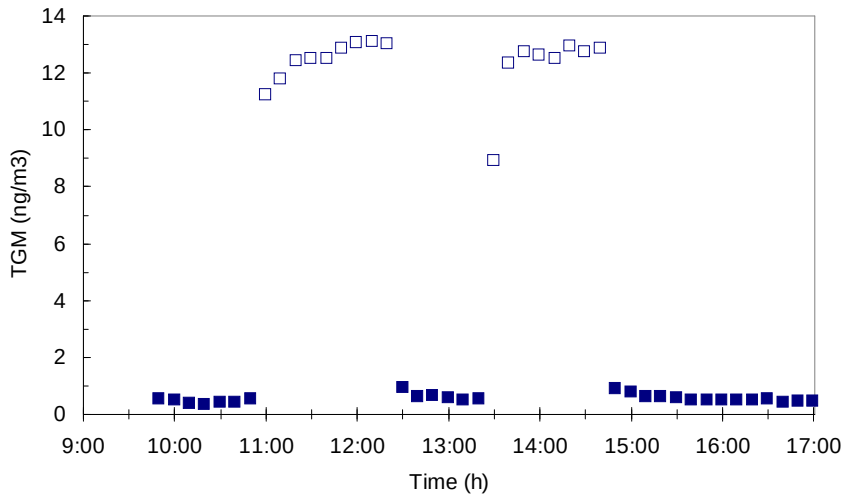

Figure 14. Effects of light on Hg emissions from unstabilized Berry's Creek sediment at 17.5 °C. TGM concentrations were measured in air passing over of a 10 cm x 100 cm sediment surface in a sealed flux chamber provided with Hg-free air in the dark (solid squares) or light (open squares).

Mercury volatilization results for Berry's Creek sediment stabilized with 6% Portland cement (dry cement weight to wet sediment weight) also show that light plays a critical role (Fig. 15). TGM concentrations in the flux chamber with cement-stabilized sediment increased in the light from 2.5 to 7.5 ng m^{-3} over the first 24 h and continued to rise to more than 20 ng m^{-3} during the next four days (Fig. 15). The surface of the cement-stabilized sediment became visually dry after four days in the flux chamber. Throughout short-term (hourly) or longer term (12 h) light-dark cycles, TGM concentrations dropped to < 0.5 ng m^{-3} in the absence of light.

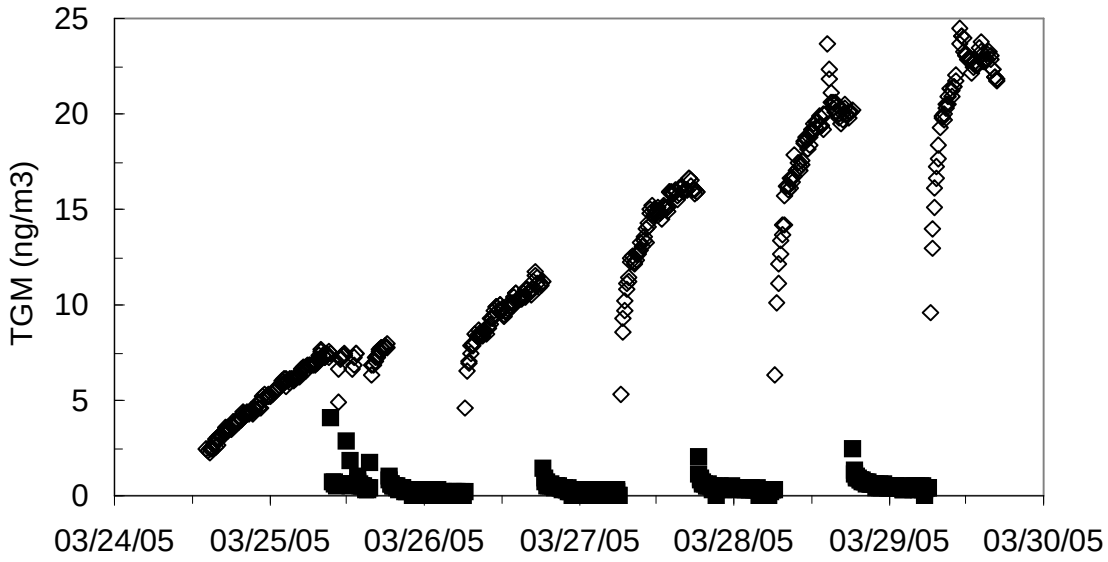

Figure 15. Effects of light on Hg emissions from cement stabilized (6% Portland cement by wet weight) Berry's Creek sediment at 17.5 °C. TGM concentrations were measured in the dark (solid squares) and light (open diamonds).

The near surface (1 cm) TGM concentrations measured in the flux chamber can be used to estimate the expected range of in situ daytime fluxes from this sediment with the modified Thornthwaite-Holtzman equation (Majewski et al., 1993).

$$F_{Hg} = \frac{u_* \kappa (Hg_1 - Hg_2)}{\ln\left(z_2 / z_1\right)\phi} \quad (1)$$

where F_{Hg} is the land-air Hg flux (ng m^{-2} h^{-1}), u_* is the friction velocity, Hg_1 and Hg_2 are the gaseous Hg concentrations (ng m^{-3}) at heights z_1 and z_2 above the ground, ϕ is the atmospheric stability correction factor, and κ is the Von Karman constant. Using the range of daytime friction velocities we measured previously at a site in Bayonne, NJ (Korfiatis et al. 2003) and assuming that background atmospheric TGM is measured at a height of 3 m and a neutral atmosphere (ϕ = 1), the estimated ranges of in situ daytime sediment-air Hg fluxes are 30-110 ng

m^{-2} h^{-1} and 620-2200 ng m^{-2} h^{-1} for unstabilized sediment in the dark (shaded) and light, respectively, and 30-90 ng m^{-2} h^{-1} and 1200-4200 ng m^{-2} h^{-1} for cement-stabilized sediment in the dark and light, respectively. The estimated fluxes of Hg from cement-stabilized Berry's Creek sediment in the light are four to ten times higher than those from SDM observed during the day at the Bayonne placement site (300-1000 ng m^{-2} h^{-1}). This is likely due to the higher concentration of Hg in Berry's Creek sediment (23 to 35 μg Hg g^{-1} dry wt) than that used in Bayonne (1.3 to 2.6 μg Hg g^{-1} dry wt). However, highly Hg enriched sediment may yield even higher Hg fluxes than those estimated in these laboratory flux chamber experiments since actual daytime irradiances at an outdoor SDM placement site are typically much higher than 80 μmol m^{-2} s^{-1} and the atmospheric stability term (ϕ) is typically less than 1 during the day due to turbulent mixing. Nonetheless, these data clearly show that light has a major effect on Hg fluxes from air-exposed sediments and suggest that further examination of the effects of the intensity and wavelength of light and sediment properties (organic matter content) on Hg volatilization from sediments across a range of Hg contamination levels is needed. These results also show that cement stabilization increases the light-driven volatilization of Hg from sediment, possibly through the greater exposure of Hg photoreactant directly to light and air through enhanced drying.

IV. References

Adams, D. A., O'Connor, J. S. and Weisberg, S. B. 1998. Sediment Quality of the NY/NJ Harbor System, US EPA.

Baker, J. E., Poster, D. L., Clark, C. A., Church, T. M., Scudlark, J. R., Ondov, J. M., Dickhut, R. M. and Cutter, G., 1997. Loadings of atmospheric trace elements and organic contaminants to the Chesapeake Bay. In: Baker, J. E., Ed. Atmospheric Deposition of Contaminants in the Great Lakes and Coastal Waters**.** SETAC Press, Pensacola, FL. pp**.**171-194.

Basu, I., Hafner, W. D., Mills, W. J. and Hites, R. A. 2004. Differences in Atmsopheric Persistent Organic Pollutant Concentrations at Two Locations in Chicago. *J. Great Lakes Res.* 30: 310-315.

Bergan, T., Gallardo, L., and Rodhe, H. 1999. Mercury in the global troposphere: a three-dimensional model study. *Atmos. Environ.* 33: 1575-1585.

Bernstein, R. L. 1982. Sea surface temperature estimation using the NOAA-6 advanced very high resolution radiometer. *J. Geophys. Res.* 87 , 9455- 9465.

Brown, J. F. 1994. Determination of PCB metabolic, excretion, and accumulation rates for use as indicators of biological response and relative risk. *Environ. Sci. Technol.* 28 (13), 2295-2305.

Brunciak, P. C., Dachs, J., Gigliotti, C. L., Nelson, E. D. and Eisenreich, S. J. 2001. Atmospheric polychlorinated biphenyl concentrations and apparent degradation in coastal New Jersey. *Atm. Env. 35*, 3325-3339.

Buehler, S. S., Basu, I. and Hites, R. A. 2001. A Comparison of PAH, PCB, and Pesticide Concentrations in Air at Two Rural Sites on Lake Superior. *Environ. Sci. Technol.* 35: 2417 -2422.

Burger, J. and Gochfeld, M. 1997. Risk, mercury levels, and birds - relating adverse laboratory effects to field biomonitoring. *Environ. Res.* 75: 160-172.

Carlson, D. L. and Hites, R.A. 2005. Temperature Dependence of Atmospheric PCB Concentrations. *Environ. Sci. Technol.* 39 , 740-747.

Cardona, T., Schaefer, J.K., Ellickson, K.M., Barkay, T., and Reinfelder, J.R. (in prep) The cycling, reduction, and volatilization of mercury in highly contaminated estuarine surface waters.

Carpi, A., Lindberg, S.E. 1997. Sunlight-mediated emission of elemental mercury from soil amended with municipal sewage sludge. *Environ. Sci. Technol.* 31:2085-2091.

Carpi, A., Lindberg, S.E. 1998. Application of a Teflon (TM) dynamic flux chamber for quantifying soil mercury flux: Tests and results over background soil. *Atmos. Environ.* 32: 873-882.

Clarkson, T.W. 2002. The three modern faces of mercury. *Environ. Health Persp.* 110(Suppl.): 11-23.

Compeau, G.C. and Bartha R. 1985. Sulfate-reducing bacteria: principal methylators of mercury in anoxic estuarine sediment. *Appl. Environ. Microbiol.* 50: 498.

Cousins, I.T., Mackay, D. 2001. Gas-Particle Partitioning of Organic Compounds and Its Interpretation Using Relative Solubilities. *Environ. Sci. Technol.* 35: 643-647.

Davies, H.C. 1976. A lateral boundary formulation for multi-level prediction models. *Quart. J. Roy. Meteor. Soc.* 102: 405-418.

Eisenreich, S.J., Looney, B.B., and Thornton, J.D. 1981. Airborne organic contaminants in the Great Lakes ecosystem. *Environ. Sci. Technol.* 15: 30-38.

Engle, M.A., Gustin, M.S., Zhang H. 2001. Quantifying natural source mercury emissions from the Ivanhoe Mining District, north-central Nevada, USA. *Atmos. Environ.* 35: 3987-3997.

Falconer, R. L. and Bidleman, T. F. 1994. Vapor pressures and predicted particle/gas distributions of polychlorinated biphenyl congeners as a function of temperature and ortho-chlorine substitution. *Atmos. Env.* 28: 547-554.

Farley, K. J., Thomann, R. V., Cooney, T. F. I., Damiani, D. R. and Wands, J. R. 1999. An Integrated Model of Organic Chemical Fate and Bioaccumulation in the Hudson River Estuary. Riverdale, NY, The Hudson River Foundation**:** 170.

Farrar, N. J., Harner, T., Shoeib, M., Sweetman, A. and Jones, K. C. 2005. Field deployment of thin film passive air samplers for persistent organic pollutants: A study in the urban atmospheric boundary layer. *Environ. Sci. Technol.* 39: 42-48.

Ferrara, R., Maserti, B.E., Andersson, M., Edner, H., Ragnarson, P., Svanberg, S., Hernandez, A. 1998. Atmospheric mercury concentrations and fluxes in the Almaden District (Spain). *Atmos. Environ.* 32: 3897-3904.

Fikslin, T. J. and Suk, N. 2003. Total Maximum Daily Loads For Polychlorinated Biphenyls (PCBs) For Zones 2 - 5 Of The Tidal Delaware River., Report to the USEPA regions II and III.

Fitzgerald, W. and Mason, R. 1996. The global mercury cycle: oceanic and anthropogenic aspects, in W. Baeyens, et al (eds.), *Global and Regional Mercury Cycles: Sources, Fluxes and Mass Balances*, 85-108, Kluwer Academic Publishers, Netherlands.

Frame, G. M., Cochran, J. W. and Boewadt, S. S. 1996. Complete PCB congener distributions for 17 Aroclor mixtures determined by 3 HRGC systems optimized for comprehensive, quantitative, congener-specific analysis. *J. High Resol. Chromatogr.* 19: 657-668.

Gigliotti, C. L., Dachs, J., Nelson, E. D., Brunciak, P. A., Eisenreich, S. J. Polycyclic Aromatic Hydrocarbons in the New Jersey Coastal Atmosphere. *Environ. Sci. Technol.* **2000**, *34*, 3547-3554.

Gigliotti, C.L., Brunciak, P.A., Dachs, J., IV, G.T.R., Nelson, E.D., Totten, L.A., Eisenreich, S.J. 2001. Air-Water Exchange of Polycyclic Aromatic Hydrocarbons in the NY-NJ Harbor Estuary. *Environ. Toxicol. Chem.* 21: 235-244.

Gilmour, C.C., Henry, E.A. and Mitchell, R. 1992. Sulfate stimulation of mercury methylation in freshwater sediments. *Environ. Sci. Technol.* 26: 2281.

Gingrich, S. E. and Diamond, M. L. 2001. Atmospherically derived organic surface films along an urban-rural gradient. *Environ. Sci. Technol.* 35: 4031-4037.

Gnamus, A., Byrne, A.R., Horvat, M. 2000. Mercury in the soil-plant-deer-predator food chain of a temperate forest in Slovenia. *Environ. Sci. Technol.* 34: 3337-3345.

Goodrow, S.M., R. Miskewitz, R.I. Hires, S.J. Eisenreich, W.S. Douglas, J.R. Reinfelder. 2005. Mercury emissions from cement-stabilized dredged material. *Environ. Sci. Technol.* 39: 8185-8190.

Goodrow S.M., R. Miskewitz, R.I. Hires, S.J. Eisenreich, W.S. Douglas, J.R. Reinfelder. 2006. *Correction to* Mercury emissions from cement-stabilized dredged material. Environ. *Sci. Technol.* 40: 409.

Gustin, M.S. 1998. NvMEP : Nevada Mercury Emissions Project-Mercury flux measurements: An intercomparison and assessment, Published Electric Power Research Institute Report, TR-111346.

Gustin. M.S. 2003. Are mercury emissions from geologic sources significant? A status report. *Sci. Total Environ.* 304: 153-167.

Gustin, M.S., G.E. Taylor, T.L. Leonard and T.E. Keislar. 1996. Atmospheric mercury concentrations associated with geologically and anthropogenically enriched sites in central western Nevada. *Environ. Sci. Technol.* 30: 2572-2579.

Gustin, M.S., S.E. Lindberg, K. Austin, M. Coolbaugh, A. Vette, and H. Zhang. 2000. Assessing the contribution of natural sources to regional atmospheric mercury budgets. *Sci. Total Environ.* 259: 61-72.

Harner, T., Bidleman, T.F. 1998. Octanol-Air Partition Coefficient for Describing Particle/Gas Partitioning of Aromatic Compounds in Urban Air. *Environ. Sci. Technol.* 32: 1494-1502.

Harner, T., Shoeib, M., Diamond, M., Stern, G. and Rosenberg, B. 2004. Using passive air samplers to assess urban - Rural trends for persistent organic pollutants. 1. Polychlorinated biphenyls and organochlorine pesticides. Environ. Sci. Technol. 38: 4474-4483.

Harrington, J. Y. (1997) The effects of radiative and microphysical processes on simulated warm and transition season Arctic stratus. Ph.D., Colorado State University.

Junge, C. E. In *Fate of Pollutants in Air and Water Environments (Part I)*, Suffett, I. H., Ed., Wiley: New York, NY, 1977.

Korfiatis, G.P., R.I. Hires, J.R. Reinfelder, L.A. Totten, and S.J. Eisenreich. 2003. Monitoring of PCB and Hg Air Emissions in Sites Receiving Stabilized Harbor Sediment. Report to the New Jersey Marine Sciences Consortium and New Jersey Department of Transportation Office of Maritime Resources.

Kozuchowski, I. and D.L. Johnson. 1978. Gaseous emissions of mercury from an aquatic vascular plant. *Nature* 274:468-469.

Lee X., Benoit G., and Hu X. Z. 2000. Total gaseous mercury concentration and flux over a coastal saltmarsh vegetation in Connecticut, USA. *Atmo. Environ.* 34: 4205-4213.

Leonard T.L., Taylor G.E., Gustin M.S., and Fernandez G.C.J. 1998. Mercury and plants in contaminated soils: 2. Environmental and physiological factors governing mercury flux to the atmosphere. *Environ. Toxicol. Chem.* 17: 2072-2079.

Lindberg, S.E., R.C. Harriss, R.R. Turner, D.S. Shriner, and D.D. Huff. 1979. Mechanisms and rates of atmospheric deposition of trace elements and sulfate to a deciduous forest canopy. ORNL/TM-6674. Oak Ridge National Laboratory, Oak Ridge, Tennessee. 510 pp.

Lindberg, S.E., Meyers, T.P., and J. Munthe. 1995a. Evasion of mercury vapor from the surface of a recently limed acid forest lake in Sweden. *Water, Air, Soil, Pollut.* 85: 725-730.

Lindberg, S.E., Kim, K.H., Meyers, T.P., and Owens, J.G. 1995b. Micrometeorological gradient approach for quantifying air-surface exchange of mercury-vapor - tests over contaminated soils. *Environ. Sci. Technol.* 29: 126-135.

Lindberg S.E., Hanson P.J., Meyers T.P., and Kim K.H. 1998. Air/surface exchange of mercury vapor over forests - The need for a reassessment of continental biogenic emissions. *Atmos. Environ.* 32: 895-908.

Lindberg, S.E., W. Dong, T. Meyers. 2002. Transpiration of gaseous elemental mercury through vegetation in a sub-tropical wetland in Florida. *Atmo. Environ.* 36: 5207-5219.

Litten, S. 2003. Contaminant Assessment and Reduction Project: Water. New York, New York State Department of Environmental Conservation**:** 158.

Lohmann, R., Nelson, E., Eisenreich, S.J., Jones, K.C. 2000. Evidence for Dynamic Air-Water Exchange of PCDD/Fs: A Study in the Raritan Bay/Hudson River Estuary. *Environ. Sci. Technol.* 34: 3086-3093.

Majewski, M., Desjardins, R., Rochette, P., Pattey, E., Seiber, J., Glotfelty, D. 1993. Field comparison of an eddy accumulation and an aerodynamic-gradient system for measuring pesticide volatilization fluxes. *Environ. Sci. Technol.* 27: 121-128.

Mason, R.P., Reinfelder, J.R., and Morel, F.M.M. 1996. Uptake, toxicity, and trophic transfer of mercury in a coastal diatom. *Environ. Sci. Technol.* 30: 1835-1845.

Mason, R.P. and Sheu, G.R. 2002. Role of the ocean in the global mercury cycle *Global Biogeochem. Cycles* 16: Art. No. 1093.

Mellor, G.L. and Yamada, T. 1982. Development of a turbulence closure model for geophysical fluid problems. Rev. Geophys. Space Phys 20 , 851-875.

Mesinger, F., Janjic, Z. I., Nickovic, S., Gavrilov, D. and Deaven, D. G. 1988. The step-mountain coordinate: Model description and performance for cases of Alpine lee cyclogenesis and for a case of Appalachian redevelopment. *Mon. Wea. Rev.* 116: 1493-1518.

Miskewitz, R., R. Hires, and G. Korfiatis. 2005. Measurement of PCB Fluxes to the Atmosphere from Stabilized Dredged Material. Report to the New Jersey Marine Sciences Consortium and New Jersey Department of Transportation Office of Maritime Resources.

Pankow, J.F. 1987. Review And Comparative Analysis Of The Theories On Partitioning Between The Gas And Aerosol Particulate Phases In The Atmosphere. *Atmos. Env.* 21: 2275.

Pankow, J.F. 1994. An absorption model of gas/particle partitioning of organic compounds in the atmosphere. *Atmos. Env.* 28: 185-188.

Poissant, L., Casimir, A. 1998. Water-air and soil-air exchange rate of total gaseous mercury measured at background sites. *Atmo. Environ.* 32: 883-893.

Rogers, E., T., Black, L., Deaven, D.G. and DiMego, G.J. 1996. Changes to the operational "Early" Eta analysis/forecast system at the national Center for Environmental Prediction. *Wea. Forecasting* 11: 391-413.

Scholtz, M.T., B.J. Van Heyst, W.H. Schroeder. 2003. Modelling of mercury emissions from background soils. *Sci. Total Environ.* 304: 185-207.

Schroeder, W.H. and Munthe, J. 1998. Atmospheric mercury—an overview. *Atmos. Environ.* 32: 809 –822.

Simcik, M.F., Franz, T.P., Zhang, H.X., Eisenreich, S.J. 1998. Gas-particle partitioning of PCBs and PAHs in the Chicago urban and adjacent coastal atmosphere: States of equilibrium. *Environ. Sci. Technol.* 32: 251-257

Stenchikov, G., Lahoti, N., Lioy, P., Georgopoulos, P., Diner, D. and Kahn, R. (submitted). Micrometeorological Pollutant Transport from the Collapse of the World Trade Center on September 11, 2001. *J. Env. Fluid Dynamics*.

Stenchikov, G., Pickering, K., DeCaria, A., Tao, W.K., Scala, J., Ott, L., Bartels, D. and Matejka, T. 2005. Simulation of the fine structure of the 12 July 1996 Stratosphere-Troposphere Experiment: Radiation, Aerosols and Ozone (STERAO-A) storm accounting for effects of terrain and interaction with mesoscale flow. *J Geophys. Res. – Atmos.* 110 (Art. No. D14304).

Totten, L.A., 2005. Present-Day Sources and Sinks for Polychlorinated Biphenyls (PCBs) in the Lower Hudson River Estuary. In: Panero, M., Boehme, S. and Muñoz, G., Eds.,

Pollution Prevention And Management Strategies For Polychlorinated Biphenyls In The New York/New Jersey Harbor**.** New York Academy of Sciences, New York. p.18.

Totten, L.A., Brunciak, P.A., Gigliotti, C.L., Dachs, J., IV, G.T.R., Nelson, E.D. and Eisenreich, S.J. 2001. Dynamic Air-Water Exchange of Polychlorinated Biphenyls in the NY-NJ Harbor Estuary. *Environ. Sci. Technol.* 35: 3834-3840.

Totten, L.A., Gigliotti, C.L., VanRy, D.A., Offenberg, J.H., Nelson, E.D., Dachs, J., Reinfelder, J.R. and Eisenreich, S.J. 2004. Atmospheric Concentrations and Deposition of PCBs to the Hudson River Estuary. *Environ. Sci. Technol.* 38: 2568-2573.

Wania, F., Haugen, J.-E., Lei, Y.D. and Mackay, D. 1998. Temperature dependence of atmospheric concentrations of semivolatile organic compounds. *Environ. Sci. Technol.* 32: 1013-1021.

Watras, C.J., Back, R.C., Halvorsen, S., Hudson, R.J.M., Morrison, K.A., and Wente, S.P. 1998. Bioaccumulation of mercury in pelagic freshwater food webs. *Sci. Total Environ.* 219: 183-208.

PCB	BAF071801AF1 surr. corrected concentration (pg/m3)	BAF071801M surr. corrected concentration (pg/m3)	BAF071901AF1 surr. corrected concentration (pg/m3)	BAF072001A surr. corrected concentration (pg/m3)	BAF072001MF1 surr. corrected concentration (pg/m3)	BAF111202A surr. corrected concentration (pg/m3)
8+5	28	0	0	13	ıo surrogate adde	0.13
18	3.6	0	2.2	0	(lab error)	0
17+15	1.6	0	1.8	0		0
16+32	2.1	0	0	8.0		0.040
31	3.0	0	0	1.8		0
28	2.0	0	0	0.75		0
21+33+53	2.5	0	0	0.61		0.0078
22	0	3.3	0	0.78		0.070
45	0	0.10	0	0		0.0025
46	0	0	0	0		0
52+43	2.3	0	2.1	1.2		0.022
49	0	0	1.4	0		0.0089
47+48	3.6	0	1.7	7.0		0.0095
44	8.7	1.8	7.2	6.7		0.020
37+42	3.2	0	4.3	1.2		0.0043
41+71	7.1	0	2.3	1.9		0
64	1.2	0	0.78	0.29		0.0045
40	0	0	0	0.89		0
74	2.4	0	3.6	0.80		0
70+76	1.5	0.80	8.4	0		0
66+95	9.3	5.1	11	3.4		0.18
91	0	0	0.56	0.47		0
56+60+89	2.2	0	3.1	1.1		0.025
92+84	3.5	0.61	3.7	1.3		0.040
101	1.6	0.37	2.5	0.92		0.029
99	1.6	5.7	0.56	3.0		0.0032
87+81	1.1	0	2.9	0.50		0.013
85+136	2.5	0.74	3.9	0.87		0.014
110+77	2.5	0.98	6.2	1.9		0.037
82	0	0	0	0.33		0.016
151	0	0	0	0.20		0
135+144+147+124	0	0	0	0.27		0
149+123+107	4.7	0.89	3.1	1.4		0.014
118	4.1	0	2.9	1.2		0.014
146	5.0	0	2.9	2.0		0.045
153+132	9.1	0	12	3.4		0.076
105	0	0	0	0		0
141+179	0.97	0	0.91	0.39		0.0081
137+176+130	0	0	1.8	0.11		0
163+138	0.72	0.042	0.54	0.22		0.00034
158	0.38	0.19	0	0.23		0.0043
187+182	2.0	1.4	5.9	0.67		0.058
183	5.3	0	1.2	0.32		0
185	0	0	0	0.078		0
174	0.50	0.31	1.2	0.37		0.0075
177	1.1	0.70	1.4	0.48		0.029
202+171+156	2.1	0	2.8	1.1		0.0031
180	1.8	1.0	1.6	0.92		0.023
199	0	0	0	0		0
170+190	0.99	0.55	1.8	0.87		0.0084
201	1.2	0.67	8.3	0.60		0.013
203+196	1.5	2.7	6.9	0.98		0.043
195+208	0.78	2.3	7.9	0.29		0.040
194	2.5	1.6	2.5	1.3		0.0088

206	1.1	1.2	15	0.34	0
surrogate recoveries *(%)*					
14	41%	0%	54%	68%	31%
23	63%	88%	64%	62%	100%
65	66%	80%	64%	63%	89%
166	77%	95%	79%	78%	98%

BAF111202M surr. corrected concentration (pg/m3)	BAF111302M surr. corrected concentration (pg/m3)	BAF111402A surr. corrected concentration (pg/m3)	BAF111402M surr. corrected concentration (pg/m3)	BAF050702A surr. corrected concentration (pg/m3)	BAF050802A surr. corrected concentration (pg/m3)	BAF050802MF1 surr. corrected concentration (pg/m3)
0.30	*0*	0.71	0.70	0.28	0.19	0.14
0	0	0.066	0	0	0.022	0.011
0	0	0	0	0	0.011	0.020
0	0	0.15	0.14	0	0.017	0
0	0	0.029	0.046	0	0.034	0.016
0	0	0.013	0.025	0	0.013	0.011
0	0	0	0.013	0	0.0039	0.010
0	0	0.10	0.28	0	0.12	0.016
0	0	0.0052	0.022	0	0.0037	0.0029
0	0	0	0.0058	0	0.0071	0
0	0	0.020	0.032	0	0.035	0.014
0	0	0	0	0	0.0072	0.010
0.11	0	0	0	0	0.017	0.0094
0	0.058	0.090	0.066	0.10	0.042	0.033
0	0.0074	0	0.012	0.0082	0.0069	0.013
0	0.043	0	0.041	0	0.031	0.013
0	0.0068	0	0.0034	0	0.0089	0.0036
0	0.0060	0	0.0066	0	0.0037	0.0034
0	0.025	0	0.047	0	0.049	0.013
0	0.053	0	0.098	0	0.085	0.038
0	0.048	0.39	0.15	0.29	0.18	0.071
0	0	0	0	0	0.0044	0.0071
0	0	0	0.026	0	0.048	0.026
0	0	0.031	0.019	0.022	0.026	0.026
0	0	0.015	0.014	0.020	0.029	0.020
0	0	0.011	0.011	0.013	0.0059	0.017
0	0	0.018	0.013	0	0.017	0.017
0	0	0.011	0.0052	0	0.014	0.013
0.051	0	0.031	0.022	0.040	0.061	0.030
0	0	0	0.0015	0	0.0068	0.0045
0	0	0.040	0.0039	0	0.018	0.0064
0	0	0.078	0	0	0.013	0.0043
0	0	0.17	0.020	0.025	0.064	0.021
0	0	0.13	0.011	0	0.061	0.018
0	0	0	0	0	0.042	0.020
0	0	0.61	0.049	0.030	0.17	0.21
0	0	0	0	0	0	0
0	0	0	0	0	0.024	0.0080
0	0	0	0	0	0.0036	0
0.011	0	0.023	0	0	0	0.0019
0.013	0	0.058	0.0036	0.0053	0.015	0.0050
0.071	0	0	0.0046	0	0.045	0.035
0	0	0	0	0	0.030	0.012
0	0	0	0	0	0.0030	0
0	0	0.093	0.0090	0	0.039	0.0082
0	0	0.18	0.0098	0	0.026	0.0087
0	0	0.084	0.0092	0	0.013	0.013
0.052	0.019	0.24	0.023	0.026	0.099	0.016
0.013	0	0	0	0	0.0021	0
0	0	0.14	0.012	0.0079	0.071	0.014
0	0	0.31	0.012	0.014	0.044	0.0092
0	0	0.64	0.016	0.018	0.057	0.017
0	0	0.34	0.0056	0.0072	0.033	0.0071
0.068	0	0.14	0.0035	0.0055	0.026	0.0094

0	0	0.23	0.0061	0	0.027	0.0066
62%	23%	50%	38%	19%	17%	66%
69%	75%	78%	83%	74%	87%	68%
64%	67%	74%	72%	80%	84%	69%
75%	85%	10%	92%	101%	110%	80%

BAF050902A surr. corrected concentration (pg/m3)	BAF050902M surr. corrected concentration (pg/m3)	BAF051002A surr. corrected concentration (pg/m3)	BAF051002M surr. corrected concentration (pg/m3)
0.067	0.16	0.037	0
0.013	0	0	0
0.015	0	0	0
0	0	0.0048	0.0091
0.020	0	0	0
0.015	0	0.0078	0
0	0	0	0
0.049	0	0.022	0
0.025	0	0	0
0	0	0	0
0.0037	0	0.0070	0
0	0	0.0015	0
0.030	0.23	0.0032	0
0.020	0.064	0.026	0.023
0	0	0.0014	0.0025
0	0.017	0	0
0.011	0.0072	0.0016	0.0025
0	0	0	0
0.0087	0.024	0	0
0	0.11	0	0
0.042	0.070	0.14	0.21
0	0	0	0
0.022	0.014	0.017	0
0.023	0.023	0.0086	0.0083
0.019	0.021	0.0043	0.010
0.036	0.011	0.0030	0.0014
0	0.012	0.0027	0.0092
0	0	0	0
0.025	0.026	0.016	0.021
0	0	0.0061	0
0	0	0	0.0025
0	0	0	0.010
0.016	0.012	0.0068	0
0	0.011	0.0053	0
0	0.032	0.0025	0.0093
0	0.037	0.024	0.035
0	0	0	0
0	0	0.0015	0.010
0	0	0	0
0.0060	0.0058	0.00059	0
0.0042	0.0047	0.0022	0
0.044	0.042	0.024	0.020
0	0	0.0011	0
0	0	0	0
0	0.0032	0.0021	0.0031
0	0.0043	0.010	0.021
0	0.0037	0	0
0.014	0.012	0.0068	0.0076
0.0072	0	0	0
0	0.027	0.0046	0.0052
0.0082	0.0076	0.0037	0.0049
0.014	0.012	0.017	0.0025
0	0	0.016	0.024
0	0	0.0039	0.0079

0	0	0.0039	0.0024
61%	36%	35%	48%
74%	64%	82%	82%
74%	67%	79%	88%
77%	107%	84%	94%

PCB	SAF071701B surr. corrected concentration (pg/m3)	SAF071801AM surr. corrected concentration (pg/m3)	SAF071801BA surr. corrected concentration (pg/m3)	SAF071801BM surr. corrected concentration (pg/m3)	SAF071801CA surr. corrected concentration (pg/m3)
8+5	5.0	6.5	24	0	0
18	1.6	1.3	13	0	0.80
17+15	0.90	0.85	15	0	0.55
16+32	2.8	1.7	19	2.8	0.38
31	3.2	2.4	56	2.5	0
28	4.5	0.85	16	1.1	0
21+33+53	1.9	1.3	5.0	1.7	0.45
22	2.5	4.8	3.4	4.6	0
45	0.082	0.092	2.8	0.077	0
46	0.24	0	41	0.55	0
52+43	2.5	1.5	36	4.7	0.90
49	2.3	1.2	35	3.9	1.4
47+48	1.9	0.79	161	4.1	1.7
44	2.0	3.0	16	3.3	2.9
37+42	1.5	0.38	7.7	0.55	1.4
41+71	3.1	2.8	47	2.9	2.4
64	1.0	0.91	4.0	0.60	0.53
40	0.31	0.29	11	0.45	0.55
74	3.0	1.9	28	0.75	1.9
70+76	29	2.6	61	3.9	2.7
66+95	9.2	8.7	9.6	25	4.9
91	0.27	0.50	23	0.53	0.33
56+60+89	3.4	2.6	28	3.0	2.4
92+84	6.6	1.6	50	2.0	1.8
101	1.2	1.5	11	2.4	1.1
99	2.7	0.31	2.2	0.58	1.8
87+81	0.77	1.0	9.6	0.59	0.62
85+136	0.16	0.85	16	2.3	1.8
110+77	2.9	4.4	41	6.3	1.7
82	0.33	0.18	1.2	0.58	1.2
151	0.52	0.32	1.1	0	0.27
135+144+147+124	0	0.51	0.94	0.39	0.55
149+123+107	2.3	2.4	4.0	2.6	1.5
118	5.5	2.8	4.2	4.4	1.4
146	2.4	1.6	2.2	1.3	1.8
153+132	5.8	5.4	12	5.6	5.1
105	0	0	0	0	0
141+179	0.61	0.63	1.0	0.55	0.55
137+176+130	0.021	0	0.29	0	0
163+138	0.17	0	1.9	0.28	0.35
158	0.67	0.63	0.88	0.62	0.32
187+182	0.95	2.0	2.3	2.6	0.52
183	0.71	0.51	1.4	0	0.73
185	0.13	0.12	0.27	0	0.14
174	1.1	0.73	1.3	0.73	0.53
177	5.0	2.7	1.0	0.56	0.29
202+171+156	0	0	1.8	0	1.1

180	2.6	2.2	2.9	1.7	0.90
199	0.039	0.046	0.073	0	0
170+190	2.4	3.0	2.9	1.6	0.63
201	1.4	1.2	1.3	0.82	0.64
203+196	1.9	3.1	1.7	2.2	0.74
195+208	1.4	2.6	1.3	2.1	0.76
194	0.89	0.68	1.1	0.61	0.33
206	1.6	1.3	1.8	0.65	0.66

surrogate recoveries *(%)*					
14	46206%	53%	99%	187%	44%
23	100%	77%	70%	74%	48%
65	99%	74%	14%	66%	48%
166	97%	79%	87%	72%	58%

SAF071801CM surr. corrected concentration (pg/m3)	SAF071901AA surr. corrected concentration (pg/m3)	SAF071901AM surr. corrected concentration (pg/m3)	SAF071901BA surr. corrected concentration (pg/m3)	SAF071901BM surr. corrected concentration (pg/m3)	SAF071901CA surr. corrected concentration (pg/m3)	SAF072001AA surr. corrected concentration (pg/m3)
0	0	0	19	35	5.4	12
0	16	18	8.8	13	2.2	3.1
0	8.1	12	6.5	8.0	1.3	1.9
0	21	17	14	18	2.3	3.2
0	46	37	16	40	4.6	2.7
0	33	34	18	28	4.4	4.2
0	29	16	14	22	2.8	2.9
0	0	26	11	43	0.24	0
0	1.5	1.5	1.6	1.9	0.20	0
0	0.94	1.5	0	5.9	0	0
0	13	17	19	16	3.4	3.1
0	10	13	15	11	2.2	2.0
0	9.8	11	14	12	1.2	1.7
1.9	14	15	18	14	3.5	5.3
0	3.8	2.7	6.6	7.1	0.75	2.2
0	13	12	16	17	3.0	5.5
0.21	5.8	7.5	5.9	7.7	1.3	1.5
0.18	2.4	1.1	3.5	2.2	0.63	0.61
0	8.2	7.2	6.7	7.6	1.5	2.3
0	24	16	22	21	5.9	5.0
8.9	31	22	38	26	11	9.1
0	1.9	0.60	3.1	0.71	0.74	0.95
1.0	19	14	19	19	4.9	4.9
1.7	7.1	4.6	10	5.7	3.5	2.6
0.87	7.0	7.7	14	8.5	3.4	2.6
0.27	12	2.5	6.4	3.8	1.4	0.98
0.26	3.7	5.4	6.7	3.2	2.0	1.1
1.7	1.4	5.7	11	0.70	6.0	1.1
3.4	13	16	22	15	6.2	5.1
0	2.0	1.0	2.5	1.3	1.8	0.98
0.27	1.5	1.9	3.1	2.1	0.82	0.78
0.098	1.4	1.0	2.2	1.4	0.82	0.47
2.0	5.8	6.9	11	6.1	3.6	3.1
1.1	9.6	16	12	17	4.0	3.8
0.80	7.8	9.9	7.6	7.1	3.0	2.8
5.0	16	16	32	14	22	9.8
0	0	0	0	0	0	0
0.48	1.8	1.6	2.8	0.65	1.0	1.1
0	1.6	0	0	0	0.40	0
0.042	12	2.4	4.3	0.12	0.75	1.3
0.52	1.8	1.8	2.8	1.4	0.87	0.51
1.5	3.4	6.6	7.2	3.5	2.5	1.8
0.49	1.7	1.5	3.1	1.5	1.1	1.4
0.057	0.57	0.18	0	0.15	0.41	0
0.78	2.0	2.1	3.7	1.3	1.2	1.1
0.65	1.5	2.0	2.5	1.8	0.91	1.2
0	4.1	0.78	0	0.80	1.3	1.7

2.3	6.2	6.2	9.2	3.7	3.5	2.8
0	0.23	0.19	0	0.12	0.13	0
2.1	5.3	5.4	8.2	2.6	3.1	2.5
1.0	3.7	3.7	6.6	3.2	1.7	1.8
2.5	4.1	5.8	7.1	5.0	2.1	2.5
2.0	1.4	3.6	2.1	4.5	2.4	1.0
1.8	1.9	2.8	5.0	2.7	2.9	1.7
0.76	4.5	6.1	15	3.4	1.9	3.1

809%	205%	374%	69%	464%	73%	66%
102%	69%	62%	59%	70%	64%	61%
91%	67%	64%	58%	69%	60%	61%
98%	80%	72%	72%	75%	71%	75%

SAF072001AM surr. corrected concentration (pg/m3)	SAF072001BA surr. corrected concentration (pg/m3)	SAF072001BA surr. corrected concentration (pg/m3)	SAF072001CM surr. corrected concentration (pg/m3)	SAF111202AA surr. corrected concentration (pg/m3)	SAF111202AM surr. corrected concentration (pg/m3)	SAF111202BA surr. corrected concentration (pg/m3)
89	9.6	0	15	0	9.4	31
28	3.7	9.6	4.1	0	3.0	0
14	2.9	5.1	2.1	0	1.7	0
34	5.6	16	5.1	0	5.3	5.3
71	5.8	21	9.7	0	10	0
58	6.6	16	4.7	0	3.5	0
48	5.9	13	8.4	1.2	4.8	4.6
33	2.3	2.3	6.4	6.7	11	2.1
2.7	0.45	1.7	1.1	0	1.7	0.30
1.9	0.88	1.6	0	0	46	0
20	7.8	15	5.2	1.5	11	2.3
17	6.8	8.1	3.5	0.86	2.4	7.1
18	5.7	6.4	2.4	0	6.2	0.83
24	7.6	13	5.1	2.1	18	1.8
7.8	2.1	4.7	1.0	0.30	1.2	0.48
25	8.4	11	5.1	0	10	0
11	2.3	4.7	1.4	0.51	3.0	0.31
5.4	1.2	2.3	0	0.28	0.83	0
13	2.4	4.7	4.7	0.42	34	0.93
35	9.4	19	14	2.1	57	0.64
45	18	37	20	12	1.3	36
2.6	1.3	4.0	1.5	0.043	11	0
30	5.1	16	5.4	2.3	18	0
10	5.1	9.7	2.7	2.8	16	0
9.2	6.4	15	4.1	2.3	0	0
9.2	2.4	16	1.1	1.5	18	0
4.2	2.0	5.9	1.6	0.77	6.2	0.41
3.8	1.9	7.7	0.75	1.7	13	0
17	10	27	8.4	5.7	27	0
3.2	1.6	3.1	0.20	0.17	4.5	0
1.9	1.4	2.9	0.77	0.60	7.8	0
1.8	1.1	2.6	1.1	0.62	22	0
7.0	5.6	11	5.6	4.4	14	1.4
12	6.8	14	11	2.5	0	0
10	4.6	8.3	1.2	10	0	2.1
21	16	31	13	12	68	5.3
0	0	0	0	0	0	0
2.3	1.6	3.3	1.6	1.3	8.1	0.21
0.95	0.47	0	0	0	0	0
14	2.0	2.7	0	0.63	132	0.30
2.2	1.5	2.9	1.4	0.96	8.1	0.61
4.3	3.4	6.9	3.4	4.5	396	3.6
2.5	1.6	2.9	2.6	1.2	56	0.41
0.52	0.30	0.69	2.5	0.049	1.5	0.060
3.0	2.0	3.2	0	1.5	14	0.83
2.1	1.4	2.2	1.7	1.6	0	1.9
5.5	2.0	5.3	0.92	0	11	0.30

8.2	5.8	8.3	7.4	3.9	40	3.0
0.20	0.14	0.30	0	0.041	0.60	0.037
7.0	4.7	6.1	5.0	2.5	33	1.1
4.5	3.5	5.9	4.0	2.0	20	2.5
5.4	3.9	5.9	4.8	5.1	19	5.5
1.9	4.3	1.7	1.5	2.8	12	3.0
2.3	1.8	2.7	1.6	0.87	9.1	1.7
4.2	6.0	13	3.0	0.83	9.5	0.71

840%	139%	403%	18%	62%	87%	49%
78%	80%	69%	81%	88%	65%	91%
77%	78%	67%	75%	74%	61%	79%
95%	96%	79%	104%	81%	61%	94%

SAF111202BM surr. corrected concentration (pg/m3)	SAF111202CA surr. corrected concentration (pg/m3)	SAF111202CM surr. corrected concentration (pg/m3)	SAF111302AM surr. corrected concentration (pg/m3)	SAF111302BA surr. corrected concentration (pg/m3)	SAF111302BM surr. corrected concentration (pg/m3)	SAF111302CA surr. corrected concentration (pg/m3)
12	11	5.7	7.1	17	7.1	8.5
1.7	0	2.4	2.7	0	0	3.8
0.56	0	0.89	1.2	0	0	1.2
1.4	0	0.81	0.22	0	0.69	0.54
3.6	0	2.7	0	0	0	6.4
0	0	1.6	0	0	0	0.64
0	0	1.3	0	0	0	0.70
7.8	0	0	0	0	0	0.87
0.098	0	0	0	0	0	0.19
0.38	0	0	0	0.58	0	0.41
2.9	0	1.2	0.53	1.0	3.5	0.85
2.4	0	3.0	1.1	0.76	1.3	0.72
0.083	0	4.4	5.0	0	11	0.45
3.5	6.7	9.8	3.0	3.0	2.8	3.3
0.51	0	0.30	0.38	0.79	1.2	0.51
0	0	3.2	1.5	1.2	2.4	2.3
1.4	0	0.64	0.44	0.43	0.57	0.41
0.38	0	0.61	0	0.36	3.5	0.34
1.5	6.7	0	1.6	2.6	2.1	2.8
4.9	14	3.9	1.9	3.0	4.1	12
17	15	8.1	2.3	4.0	5.5	3.3
0.10	1.3	0.62	0	0.44	0	0.18
3.8	5.5	6.4	1.4	1.6	2.3	1.6
2.3	2.5	3.9	1.9	2.0	2.2	1.7
2.4	2.3	2.5	1.0	1.0	1.1	1.0
0.47	0.93	12	4.1	1.3	2.1	2.6
0.94	1.0	1.6	0.45	1.1	0.72	0.64
0.93	0	0	0.76	2.8	0.80	1.5
7.1	5.1	6.3	1.4	2.0	1.4	1.9
0.50	0	0.95	0.17	0.38	0	0.27
0.95	0.45	1.8	0.29	0.43	0	0.35
0.83	0	5.1	0.48	0.23	0	0.25
3.9	2.9	0	1.0	1.1	1.1	0.99
6.5	13	4.4	1.2	0.91	0.87	1.2
8.0	8.1	0	4.1	3.1	3.5	1.6
11	6.2	6.0	3.0	3.1	4.1	3.5
0	0	0	0	0	0	0
1.2	0.78	1.1	0.42	0.44	0.38	0.32
0	0	0	0	0	0	0
0.12	0.64	1.6	0.33	1.0	0.87	0.20
1.1	0.77	1.2	0.24	0.24	0.22	0.22
4.0	5.6	103	1.4	0.88	1.1	1.9
0.98	0	0	0.36	0.46	0.30	0.34
0.11	0	0	0	0	0	0
1.5	1.3	1.6	0.47	0.39	0.50	0.46
2.4	2.3	0	0.49	0.54	0.37	0.34
0.66	4.6	0	0.36	0.74	2.6	0.52

4.5	2.9	4.5	0.89	0.90	0.66	0.87
0.11	0	0	0	0.065	0	0
3.6	2.5	3.4	0.49	0.61	0.74	1.1
3.6	2.0	5.0	0.50	0.87	0.79	0.61
5.9	2.1	3.2	0.81	0.64	0.83	0.75
2.9	0	0	0.26	0.19	2.3	0.33
1.6	0.57	5.2	0.20	0.47	1.1	0.64
1.4	1.7	3.3	0.23	0.46	0.51	0.29

51%	60%	69%	75%	73%	74%	78%
87%	66%	63%	77%	74%	76%	71%
82%	67%	57%	75%	66%	74%	64%
88%	74%	57%	95%	72%	98%	76%

SAF111302CM surr. corrected concentration (pg/m3)	SAF111402AA surr. corrected concentration (pg/m3)	SAF111402AM surr. corrected concentration (pg/m3)	SAF111402BA surr. corrected concentration (pg/m3)	SAF111402BM surr. corrected concentration (pg/m3)	SAF111402CA surr. corrected concentration (pg/m3)	SAF111402CM surr. corrected concentration (pg/m3)
16	0.015	26	25	67	17	47
0	0	3.5	6.5	2.0	8.0	1.2
0	0	0.45	0.35	4.5	4.0	2.6
1.2	0.00070	2.0	4.0	7.8	0.82	6.0
0	0.0018	1.5	1.9	4.2	0	0
0	0.0011	0.56	0	0	0	0
1.3	0.00089	0	0	0.95	0.85	0
0	0.0024	0.54	0	16	0	11
0	0.000045	0	0	1.2	0	0
0	0	0	0	0.62	0	0
1.3	0.0012	0.55	1.6	3.2	1.4	2.7
0.61	0.00039	0.60	0.92	3.1	0.46	0
1.3	0.0013	0	0.82	0	0.49	0
2.5	0.0010	1.1	2.1	5.7	1.4	0
0.52	0.00031	0.26	0.94	0.91	0.47	0
3.1	0	2.8	2.2	1.4	0.95	0
0.42	0.00024	0.29	0.54	0.37	0.39	0
0	0	0	0.32	0.23	0.27	0
0	0.00034	0.54	1.1	3.8	0.73	0
0	0.0063	0.75	2.9	13	1.5	0
6.9	0.0029	1.6	4.2	12	3.5	6.3
0	0	0	0.57	0.39	0.23	0
0.85	0.00032	0.58	1.9	2.6	0.98	1.4
0.98	0.0016	1.2	2.5	1.8	1.4	1.7
1.0	0.00085	0.58	1.6	2.1	0.88	1.1
0.38	0.00091	0.35	0.52	1.0	0.43	0
0.41	0.00030	0.60	0.68	1.4	1.1	0
0	0.00017	0.19	0.61	0.38	1.2	0
1.3	0.0023	1.6	2.9	5.4	1.8	1.6
0.14	0	0.20	0.46	0.33	0.32	0
0.31	0.00020	0.32	0.54	0.98	0.38	0
0.36	0.00019	0	0.36	0	0.29	1.2
1.2	0.0012	1.2	2.0	3.4	1.4	0
0	0.0011	1.2	1.5	6.6	1.1	0
0.29	0.0028	0	2.2	1.8	1.6	0
4.3	0.0046	3.6	5.5	8.7	4.3	5.7
0	0	0	0	0	0	0
0.71	0.00049	0.37	0.53	1.1	0.41	0
0	0	0	0	0.16	0.16	0
0	0.00011	0.33	0.46	0	0.23	0
0.37	0.00043	0.32	0.41	0.76	0.28	0.43
0.26	0.0015	0.93	0.93	0.63	1.5	0.65
0.47	0.00035	0.59	0.67	0.97	0.45	0.59
0	0.000057	0.11	0.089	0.18	0.079	0
0.57	0.00083	0.34	0.60	0	0.58	0.97
0.47	0.00092	0.054	0.51	1.0	0.47	1.4
0.36	0.00020	0.54	0.61	0.65	0.54	0

1.4	0.0016	1.7	1.4	2.9	1.2	1.9
0	0.000022	0	0	0.11	0	0
0.27	0.0014	1.1	1.1	0	1.1	0.48
0.57	0.00086	0.96	0.75	1.2	0.76	1.4
0.97	0.0018	1.2	1.2	1.6	1.1	1.8
0	0.0019	0.34	0.39	0.54	1.0	0.16
0.65	0.00049	1.6	1.2	0.43	0.52	0.33
0	0.00077	0.41	0	0.41	0.49	0.97

48%	4747%	105%	82%	41%	73%	16%
74%	91%	78%	73%	80%	78%	59%
77%	85%	66%	67%	72%	74%	62%
94%	91%	81%	79%	92%	78%	73%

SAF050702AM surr. corrected concentration (pg/m3)	SAF050702BA surr. corrected concentration (pg/m3)	SAF050702BM surr. corrected concentration (pg/m3)	SAF050702CA surr. corrected concentration (pg/m3)	SAF050702CM surr. corrected concentration (pg/m3)	SAF050802AA surr. corrected concentration (pg/m3)	SAF050802AM surr. corrected concentration (pg/m3)
14	3.6	6.8	12	14	11	9.2
4.1	1.1	4.7	0.74	0	2.8	3.6
3.1	0.63	0	0.43	0	1.4	2.3
2.1	1.2	4.0	0.37	5.3	1.8	4.2
9.0	3.2	7.6	0	0	8.4	8.3
5.6	0	6.7	0	0	8.5	9.5
0	1.0	2.5	0	0.92	2.5	2.5
5.7	4.9	9.7	0	3.1	0	1.7
0.92	0.14	0.36	0	0	0	0.17
0	0.41	0.36	0.46	0.24	0.081	0.60
3.2	2.6	5.9	0.63	0.82	6.6	4.9
1.1	0.98	3.2	0.39	0.21	4.5	3.8
2.2	1.8	2.9	1.8	0.50	13	2.9
4.0	3.1	5.7	6.0	2.0	7.5	6.1
0.60	0.55	1.1	1.4	0.19	1.0	1.7
4.0	1.6	5.6	2.2	0	7.3	5.0
1.0	0.77	1.8	0.50	0.20	2.8	2.2
0.47	0.43	0.61	0.38	0.15	0.68	1.2
0.67	3.2	6.4	1.5	0	4.2	3.3
6.3	4.4	14	1.3	0	11	9.5
9.3	9.6	28	4.6	7.7	15	16
0.48	0.54	1.5	0	0	2.7	1.3
5.0	3.3	9.1	1.9	0.92	11	8.5
2.2	1.9	4.2	1.5	0.91	7.3	5.3
2.4	2.5	5.4	1.2	0.74	6.8	4.8
1.4	0.56	2.1	0.44	0.16	9.0	2.1
0.91	1.0	2.1	2.9	0.53	4.8	2.4
0.34	0.40	0.73	4.9	0.48	1.6	9.3
4.8	5.4	12	2.0	1.9	14	8.9
0.57	0.52	0.97	0.50	0	0.75	1.2
1.1	1.5	2.2	1.0	0.37	1.6	1.3
0.60	1.3	1.9	0.46	0.25	0.19	1.0
3.4	5.4	8.3	2.1	1.4	4.8	5.2
5.3	4.9	14	1.1	0.91	6.0	5.3
1.2	2.2	4.9	1.1	0.68	7.2	3.8
9.4	13	20	10	3.8	14	15
0	0	0	0	0	0	0
1.3	1.8	3.2	0.60	0.45	1.5	1.5
0	0.22	0.14	0	0	0.092	0
0	0	0.033	0.28	0.020	3.9	0.44
0.81	1.2	2.0	0.40	0.29	1.3	1.2
1.3	4.2	4.9	3.5	1.7	8.2	4.0
1.2	2.1	3.1	0.54	0.25	1.7	1.7
0.28	0.46	0.83	0	0	0.28	0.25
1.8	2.9	3.8	0.87	0.61	2.3	2.0
1.2	1.8	2.4	1.7	2.1	2.1	1.3
0.87	1.4	2.1	0	0	0.41	2.6

5.2	7.5	10	2.0	1.7	6.4	4.7
0.11	0.19	0.25	0	0	0.096	0.21
3.4	5.0	7.1	2.9	1.6	5.6	3.8
2.8	5.9	7.6	1.5	1.1	3.5	2.9
3.4	5.7	7.7	2.0	2.7	4.4	3.2
1.1	1.4	2.0	0.78	1.9	4.0	0.99
1.3	1.9	2.8	0.92	1.4	2.3	1.2
2.4	17	22	0.87	1.0	4.5	2.7

25%	24%	49%	50%	0%	0%	51%
86%	72%	91%	55%	103%	51%	55%
81%	73%	83%	53%	85%	53%	52%
104%	100%	112%	50%	95%	89%	67%

SAF050802BA surr. corrected concentration (pg/m3)	SAF050802BM surr. corrected concentration (pg/m3)	SAF050802CM surr. corrected concentration (pg/m3)	SAF050902AA surr. corrected concentration (pg/m3)	SAF050902AM surr. corrected concentration (pg/m3)	SAF050902CA surr. corrected concentration (pg/m3)	SAF050902CM surr. corrected concentration (pg/m3)
	12	21	2.6	6.9	9.3	3.8
	2.3	0	0.61	0	0	0
	1.2	0	0.52	0	0	0
	2.1	6.4	0	1.7	0.17	0.42
	6.6	0	0	0	0	0
	4.0	0	0	0	0	0
	1.0	3.4	0	0.95	0	0
	7.1	4.1	0	2.2	1.0	0
	0.78	0.44	0	0	0	0
	0	0	0	0	0	0
	2.4	1.9	1.6	0.53	0.26	0.93
	1.2	0.27	0.87	0.42	0.10	0.70
	5.6	0	16	0	0	2.0
	8.4	2.0	0	1.5	0.52	2.3
	0.98	0.25	0	0.19	0.12	0
	2.8	0	0	0	0	0
	0.62	0.21	0	0.20	0.14	0.83
	0.67	0.18	0	0	0	0
	7.1	0.48	4.3	0	0	0
	10	0.40	5.9	0	0.17	0.83
	12	5.5	11	8.7	4.1	3.6
	1.2	0	0	0	0	0
	6.4	1.0	5.6	0.71	0.13	1.3
	2.3	1.5	3.8	1.1	0.52	1.2
	2.7	0.97	4.0	1.2	0.42	1.1
	1.4	0.45	11	1.2	0.11	0.75
	1.7	0.49	2.5	0.47	0.36	0.47
	1.1	0.29	0	0.28	0.088	0.44
	7.1	2.3	12	3.0	1.6	2.3
	0.72	0.46	1.6	0	0.11	0.40
	1.0	0	1.5	0.20	0.26	0.54
	0	0.13	1.2	0	0.11	0.22
	3.2	1.4	3.9	1.5	0	1.3
	11	1.1	20	2.3	0	0.93
	2.0	0.45	12	8.7	1.5	2.6
	10	3.8	17	4.7	2.9	4.5
	0	0	0	0	0	0
	1.3	0	1.6	0.54	0.14	0
	0	0	0	0	0	0
	1.0	0.097	3.9	0.045	0.017	0.53
	1.3	0.46	2.3	0.49	0.27	0.37
	0	1.5	2.0	2.0	1.7	0.90
	0	0.49	1.1	0.28	0.14	0.11
	0	0	0.19	0	0	0.086
	1.7	0.58	1.6	0.38	0.27	0
	2.8	0.92	1.3	1.3	1.1	0.32
	4.6	0	0.78	0.14	0.12	0

4.4	1.7	4.4	1.1	0.73	1.4
0	0.39	0	0	0	0
3.8	1.3	4.4	0.50	0.60	1.0
3.2	1.2	1.5	0.50	0.31	0.56
3.6	2.6	1.6	2.2	1.8	0.60
2.3	1.7	1.6	1.6	1.4	0.17
0.94	0.75	2.3	0.33	0.41	8.3
4.4	1.1	1.5	0.12	0.089	0.070

62%	55%	79%	43%	0%	54%
74%	93%	71%	80%	63%	70%
71%	81%	75%	75%	74%	65%
71%	101%	88%	84%	96%	76%

SAF051002BA surr. corrected concentration (pg/m3)	SAF051002BM surr. corrected concentration (pg/m3)	SAF051002CA surr. corrected concentration (pg/m3)	SAF051002CM surr. corrected concentration (pg/m3)
4.6	5.7	0	3.1
0	0	0	0
0	0	0	0
0.79	1.1	0.83	0.42
0	1.7	2.5	0.93
0	0.44	0	0.13
0	1.3	0.076	0.25
0	4.1	3.1	2.6
0	0.18	0	0.073
0	0.28	0	0
0.81	1.6	0.67	0.23
0.32	0.35	0.22	0
0.68	0.47	0.26	0
2.7	2.3	3.5	0.67
0.48	0.72	0.20	0.18
1.4	0	0	0
0.36	0.18	0.11	0.11
0	0.11	0	0
0	0	0.50	0
0.70	0	1.8	0
16	11	6.8	4.5
0.087	0	0	0
0.95	1.3	0.64	0.65
0.92	0.96	0.63	0.81
1.2	0.90	0.49	0.47
0.38	0.32	0.35	0.11
0.31	0.67	0.27	0.42
0.24	0.61	0.23	0.44
2.2	2.8	1.5	1.6
0	0.17	0.10	0.12
0.23	0.40	0.25	0.29
0.30	0.37	0.18	0.26
1.9	1.6	0.93	0.90
1.1	1.5	0.66	0.88
1.0	1.0	0.36	1.0
4.9	4.3	2.9	2.5
0	0	0	0
0.56	0.49	0.29	0.23
0	0	0.039	0
0	0	0.052	0.025
0.44	0.37	0.20	0.23
2.6	1.8	1.8	1.6
0.61	0.37	0.31	0.19
0.095	0.077	0.054	0
0.76	0.65	0.49	0.26
1.2	2.1	1.3	1.3
0.51	0.32	0	0.066

2.1	1.7	1.0	0.71
0.068	0.044	0	0.035
1.5	1.3	0.91	0.74
1.6	1.0	0.49	0.39
3.3	2.9	1.9	1.6
3.3	2.5	1.6	1.6
0.78	0.81	0.72	0.92
4.0	2.0	0.34	0

48%	18%	58%	22%
72%	90%	81%	76%
75%	77%	80%	78%
89%	83%	87%	84%

	LAB BLANK	LAB BLANK	LAB BLANK	LAB BLANK	LAB BLANK	LAB BLANK
	LBF071604F1	LBF010405F1	LBF010605F1	LB033005	LB042105	LB042905
PCB	surr. corrected mass (pg)	surr. corrected mass (pg)	surr. corrected mass (pg)	surr. corrected mass (pg)	surr. corrected mass (pg)	surr. corrected mass (pg)
8+5	0	0	0	264	0	0
18	0	0	0	0	0	0
17+15	0	0	0	0	0	0
16+32	0	0	0	0	0	0
31	0	0	0	0	0	0
28	0	0	0	0	0	0
21+33+53	0	0	0	0	0	0
22	0	0	0	0	0	0
45	0	0	0	0	0	0
46	0	0	0	0	0	0
52+43	0	0	0	0	0	0
49	0	0	0	0	0	0
47+48	0	0	0	5800	0	0
44	0	0	0	0	0	0
37+42	0	0	0	0	0	0
41+71	0	0	0	0	0	0
64	0	0	0	0	0	0
40	0	0	0	0	0	0
74	0	0	0	0	0	0
70+76	0	0	0	0	0	0
66+95	0	0	0	0	0	0
91	0	0	0	0	0	0
56+60+89	0	0	0	0	0	0
92+84	0	0	0	0	0	0
101	0	0	0	0	0	0
99	0	0	0	0	0	0
87+81	0	0	0	0	0	0
85+136	0	0	0	0	0	0
110+77	0	0	0	0	0	0
82	0	0	0	0	0	0
151	0	0	0	0	0	0
135+144+147+124	0	0	0	0	0	0
149+123+107	0	0	0	0	0	0
118	0	0	0	0	0	0
146	0	0	0	0	0	0
153+132	0	0	0	0	0	0
105	0	0	0	0	0	0
141+179	0	0	0	0	0	0
137+176+130	0	0	0	0	0	0
163+138	0	0	0	0	0	0
158	0	0	0	0	0	0
187+182	0	0	0	0	0	0
183	0	0	0	0	0	0
185	0	0	0	0	0	0
174	0	0	0	0	0	0
177	0	0	0	0	0	0
202+171+156	0	0	0	0	0	0
180	0	0	0	0	0	0
199	0	0	0	0	0	0
170+190	0	0	0	0	0	0
201	0	0	0	0	0	0
203+196	0	0	0	0	0	0
195+208	0	0	0	0	0	0
194	0	0	0	0	0	0
206	0	0	0	0	0	0

surrogate recoveries *(%)*						
14	58%	56%	0%	80%	0%	0%
23	58%	65%	37%	60%	63%	66%
65	65%	68%	49%	67%	78%	79%
166	71%	76%	60%	62%	76%	91%

LAB BLANK	LAB BLANK	LAB BLANK	LAB BLANK	FIELD BLANK	FIELD BLANK
LB051805	LB052305	LB052505	LB052805	BAF071801FB	BAF050602FBF1
surr. corrected mass (pg)	surr. corrected mass (pg)	surr. corrected mass (pg)	surr. corrected mass (pg)	surr. corrected mass (pg)	surr. corrected mass (pg)
0	0	0	0	0	0
0	0	0	0	0	109
0	0	0	0	0	57
0	0	0	0	0	0
0	0	0	0	0	0
0	0	0	0	0	0
0	0	0	0	0	0
0	0	0	0	0	0
0	0	0	0	0	0
0	0	0	0	0	0
0	0	0	0	0	153
0	0	0	0	0	0
0	0	0	0	0	92
0	0	0	0	0	467
0	0	0	0	0	185
0	0	0	0	0	0
0	0	0	0	0	0
0	0	0	0	0	0
0	0	0	0	0	561
0	0	0	0	0	0
1186	1301	877	838	798	271
0	0	0	0	0	0
0	0	0	0	0	0
0	0	0	0	0	0
0	0	0	0	0	0
0	0	0	0	0	0
0	0	0	0	0	0
0	0	0	0	0	0
0	0	0	0	0	0
0	0	0	0	0	0
0	0	0	0	0	0
0	0	0	0	0	0
0	0	0	0	0	0
0	0	0	0	0	0
0	0	0	0	0	0
0	0	0	0	0	0
0	0	0	0	0	0
0	0	0	0	0	0
0	0	0	0	0	0
0	0	0	0	0	0
0	0	0	0	0	0
0	629	0	478	0	0
0	0	0	0	0	0
0	0	0	0	0	0
0	0	0	0	0	0
225	229	163	192	0	199
0	0	0	0	0	0
0	0	0	0	0	0
0	0	0	0	0	0
0	0	0	0	0	0
0	0	0	0	0	0
429	447	316	315	0	346
334	340	243	262	0	263
0	0	0	0	0	0
0	0	0	0	0	0

0%	0%	0%	0%	64%	0%
47%	49%	80%	80%	68%	90%
64%	79%	100%	93%	65%	72%
72%	72%	92%	83%	76%	87%

FIELD BLANK	FIELD BLANK	FIELD BLANK	FIELD BLANK	FIELD BLANK	FIELD BLANK	FIELD BLANK
BAF050802FB	BAF050902FB	BAF111202FB	BAF111302FB	BAF111402FBF1	SAF050602FBF1	SAF050802FB
surr. corrected mass (pg)	surr. corrected mass (pg)	surr. corrected mass (pg)	surr. corrected mass (pg)	surr. corrected mass (pg)	surr. corrected mass (pg)	surr. corrected mass (pg)
0	647	0	425	0	0	0
0	0	0	0	0	0	0
0	0	0	0	0	0	0
0	0	0	0	0	0	0
0	0	0	0	0	0	1020
0	0	0	0	0	0	283
0	0	0	0	0	0	1276
0	0	0	0	0	0	0
0	0	0	0	0	0	0
0	0	0	0	0	0	0
0	0	0	0	0	0	0
0	0	0	0	0	0	0
0	2913	0	0	0	0	0
0	1314	0	0	0	0	153
0	0	0	0	0	0	0
0	0	0	0	0	0	0
0	0	0	0	0	0	0
0	0	0	0	0	0	0
0	0	0	0	0	0	0
0	0	0	0	0	0	0
0	0	736	0	0	0	0
0	0	0	0	0	0	0
0	0	0	0	0	0	0
0	0	0	0	0	0	0
0	0	0	0	0	0	0
0	0	0	0	0	0	0
0	0	0	0	0	0	0
0	0	0	0	0	0	0
0	0	0	0	0	0	0
0	0	0	0	0	0	0
0	0	0	0	0	0	0
0	0	0	0	0	0	0
0	0	0	0	0	0	0
0	0	0	0	0	0	0
0	0	0	0	0	0	0
0	0	0	0	0	0	0
0	0	0	0	0	0	0
0	0	0	0	0	0	0
0	0	0	0	0	0	0
0	0	0	0	0	0	0
4673	485	0	0	0	2756	0
0	0	0	0	0	0	0
0	0	0	0	0	0	0
0	0	0	0	0	0	0
0	219	0	0	0	0	0
0	0	0	0	0	0	0
0	0	0	0	0	0	0
0	0	0	0	0	0	0
0	0	0	0	0	0	0
0	0	0	0	0	0	0
0	409	0	0	0	0	0
0	299	0	0	0	0	0
0	0	0	0	0	0	0
0	0	0	0	0	0	0

59%	0%	0%	0%	55%	73%	51%
55%	71%	64%	58%	67%	60%	67%
58%	75%	60%	62%	66%	62%	70%
1511%	76%	75%	74%	85%	151%	75%

FIELD BLANK	FIELD BLANK	FIELD BLANK	FIELD BLANK	MATRIX SPIKE	MATRIX SPIKE
SAF050902FB	SAF051002FB	SAF111202FB	SAF111402FB	MSF071604F1	MSF010605F1
surr. corrected mass (pg)	surr. corrected mass (pg)	surr. corrected mass (pg)	surr. corrected mass (pg)	surr. corrected mass (pg)	surr. corrected mass (pg)
392	0	4635	0	5739	4244
0	0	0	0	1462	1404
0	0	0	0	890	826
0	0	0	0	1402	1405
0	0	0	0	2041	1263
0	0	0	0	1992	2016
0	0	0	0	2046	1528
0	0	0	0	1295	622
0	0	513	0	314	200
0	0	0	0	182	199
0	0	0	0	1471	1591
0	0	0	0	1026	1040
8280	0	0	0	969	934
0	0	288	0	2021	1820
0	0	0	0	752	674
0	0	0	0	1792	1095
0	0	0	0	963	777
0	0	0	0	493	315
0	0	0	0	1154	582
0	0	0	0	2740	1450
0	0	0	7280	3328	1934
0	0	0	0	185	156
0	0	0	0	2234	1640
0	0	0	0	581	775
0	0	0	0	574	629
0	0	0	0	349	256
0	0	0	0	326	176
0	0	0	0	594	760
0	0	0	0	964	771
0	0	0	0	223	146
0	0	0	0	772	662
0	0	0	0	370	273
0	0	0	0	1660	1480
0	0	0	0	369	412
0	0	0	0	223	135
0	0	0	0	3096	3000
0	0	0	0	0	0
0	0	0	0	791	620
0	0	0	0	322	318
0	0	0	0	618	408
0	0	0	0	156	130
0	0	0	0	2315	2025
0	0	0	0	1160	937
0	0	0	0	249	308
206	0	0	0	1662	1387
0	0	0	0	921	692
0	0	0	0	497	441
0	0	0	0	3536	2493
0	0	0	0	148	114
0	0	0	0	1819	1328
0	0	0	0	2317	1770
378	0	0	0	2659	2002
302	0	0	0	1261	931
199	0	0	0	1078	874
0	323	0	0	924	626

0%	0%	8%	8%		104%	1743%
70%	70%	82%	82%		67%	61%
79%	68%	71%	71%		72%	75%
80%	84%	86%	86%		57%	79%

MATRIX SPIKE	MATRIX SPIKE	MATRIX SPIKE	MATRIX SPIKE	MATRIX SPIKE
MS030305	MS042105	MS042905	MS052305	MS052805
surr. corrected mass (pg)	surr. corrected mass (pg)	surr. corrected mass (pg)	surr. corrected mass (pg)	surr. corrected mass (pg)
6936	0	6489	0	0
1902	2098	2458	1886	2084
1010	1168	1382	1090	1093
1691	1885	2404	2348	2418
3580	1348	0	16828	0
2374	0	0	0	2980
3012	0	497	2183	1392
2283	0	0	1674	0
370	302	341	260	251
2406	236	204	0	0
2423	2515	2361	2282	2154
1252	1719	1607	1516	1582
3500	1747	1619	1610	1606
2816	2878	2797	2577	2476
615	696	664	676	563
2117	1675	1893	0	0
1025	1189	1233	1313	1451
502	405	594	0	485
6542	1565	1381	1852	0
4783	2452	3447	5312	2395
4630	3064	5152	13495	3995
0	243	318	0	0
3483	1916	1830	3332	5110
707	755	954	628	0
759	869	771	857	870
205	334	403	475	0
629	189	247	445	467
1996	154	352	566	557
1541	1137	1179	1384	1277
43	254	205	259	0
146	1077	1095	1089	1157
322	434	477	504	446
0	2387	2214	2243	2111
93	452	0	516	0
0	216	432	131	153
526	3992	4050	3966	3930
0	0	0	0	0
145	1126	0	1094	987
0	347	378	290	0
62	0	15	0	181
32	220	209	237	224
5732	2888	2741	2595	2429
1225	1707	1588	1646	1552
44	493	383	391	426
294	2405	2232	2151	2078
216	1182	1117	1145	1124
136	804	751	602	679
667	5018	4474	4929	4309
26	220	203	197	189
341	2140	2024	2348	2289
433	3216	2825	3044	2820
498	3442	3070	3430	3231
240	1580	1441	1573	1577
209	1226	1104	1476	1320
148	955	646	961	834

64%	0%	0%	0%	0%
66%	51%	63%	77%	73%
72%	68%	73%	90%	80%
438%	81%	91%	85%	81%